# CHARACTERIZATION OF THE *SACCHAROMYCES CEREVISIAE RAD5* GENE AND PROTEIN

A Thesis Submitted to the College of

Graduate Studies and Research

In Partial Fulfillment of the Requirements

For the Masters of Science

In the Department of Microbiology and Immunology

University of Saskatchewan

Saskatoon

By

SUSAN BLACKWELL

## PERMISSION TO USE

In presenting this thesis in partial fulfillment of the requirements for a Postgraduate degree from the University of Saskatchewan, I agree that the libraries of this University may make it freely available for inspection. I further agree that permission for copying of this thesis in any manner, in whole or in part, for scholarly purposes may be granted by the professor or professors who supervised my thesis work or, in their absence, by the Head of the Department or the Dean of the College in which my thesis work was done. It is understood that any copying or publication or use of this thesis or parts thereof for financial gain shall not be allowed without my written permission. It is also understood that due recognition shall be given to me and to the University of Saskatchewan in any scholarly use which may be made of any material in my thesis

Requests for permission to copy or to make other use of material in this thesis in whole or part should be addressed to:

Head of the Department of Microbiology and Immunology
University of Saskatchewan
Saskatoon, Saskatchewan S7N 5E5
Canada

## ABSTRACT

DNA damage tolerance (DDT) is a process utilized by cells to bypass replication blocking lesions in the DNA, preventing replication fork collapse and maintaining genomic stability and cell viability. In *Saccharomyces cerevisiae* DDT consists of two branched pathways. One branch allows direct replication past lesions in the DNA utilizing specific error-prone polymerases, a process known as translesion DNA synthesis (TLS). The other branch utilizes homologous recombination and template switch to replicate past damaged DNA in an error-free manner.

*RAD5* has traditionally been characterized as belonging to the error-free pathway of DNA damage tolerance. The protein is multi-functional, with several specific activities identified and classified to the error-free branch of DDT. However, there is also evidence for additional uncharacterized activities of the protein. The goal of this research was to determine which branches of DNA damage tolerance the uncharacterized activities of Rad5 are involved in. A two-pronged approach was utilized, elucidation of the physical interactions of the protein, and examination of the genetic interactions between *RAD5* and other DDT genes.

The evidence indicates that Rad5 plays a partial role in TLS and the protein is known to physically interact with Rev1, a member of the TLS pathway. We assumed this physical interaction mediates the TLS activity of Rad5. The yeast two-hybrid assay was utilized to examine the interaction between Rev1 and truncated Rad5 fragments, and the N-terminal 30 amino acids of Rad5 proved sufficient to maintain the interaction. This research sets the stage to identify key residues in Rad5 for the interaction with Rev1, and the creation of a TLS deficient *rad5* mutant by targeting those key residues.

Genetic interactions between *RAD5* and genes required for the initiation of DDT in the cell were examined based on sensitivity to killing by various DNA damaging agents. We determined that the functions of Rad5 rely on PCNA modification, and thus do not function in a cellular process unrelated to Rad5. Potential uncharacterized functions are discussed on the basis of these results and the results of the interaction studies. Future structural and functional studies are proposed to better understand the role of Rad5 in the cell.

ACKNOWLEDGEMENTS

I would like to thank everyone who has helped me along the way to achieving a Master's degree. I wouldn't have made it this far without any of you, so thank you!

I would like to thank Dr. Wei Xiao, my supervisor, for providing me with the opportunity to work in his lab. I have constantly been challenged to expand my skills and knowledge, and I have undoubtedly learnt more from him than I even realize at this time. I am grateful for the chances you gave me as both an undergraduate and a graduate student.

I would like to thank my committee members, Dr. Stan Moore, Dr. Hughes Goldie, Dr. Kerri Kobryn and Dr. Michel Desautels. Thank you for giving your time and guidance while I worked toward this goal.

A huge thank you to everyone I have ever worked with in the Wei Xiao laboratory. I particularly wish to thank Parker Andersen, Landon Pastushok, Audesh Bhat, Lindsay Ball, Jia Li, Sheng Wang, Rui Wen, Hanna Dworaczek and Michael Biss. Most of all, I would like to thank Michelle Hanna and Amanda Lambrecht not only for their assistance with my work, but for also providing an unwavering friendship. Thank you all for your technical assistance and willingness to discuss my project at any time. Thank you!

Thank you to those who work within the department of Microbiology and Immunology and now Biomedical Sciences. I want to give a special thanks to Mary, Dawn, Cindy, Vern, Katie, Heather, Sherry and Corrine.

To my parents, thank you! You have pushed me to never stop questioning and to always keep learning and pushing for more. I have no doubt that it is these values that you instilled in me that have led me on this path, and I can only hope that I have lived up to your expectations. Thank you! To my twin, Jesse, I rely on your support more than anyone else. I am forever

grateful for your shoulder to lean on whenever I doubted myself. I will always appreciate your willingness to listen to me ramble on about science. To the rest of my friends and family, thank you for your never ending love and support. Thank you for helping me stay focused and never letting me give up.

Last and most of all I would like to thank my partner Kris. Your encouragement, patience, support and love have sustained me throughout my academic career. Thank you for putting up with me through it all, and I am incredibly lucky to have you by my side. Thank you!

TABLE OF CONTENTS

page

LIST OF TABLES

page

LIST OF FIGURES

page

# LIST OF ABBREVIATIONS

Abbreviation

°C…….Degrees celsius

Δ……...Deletion mutant (null mutation)

%**.....**Percentage

3AT……..3-amino triazole

Ade……..Adenine

Amp…….Ampicillin

APS……..Ammonium persulfate

ATP……..Adenosine triphosphate

ATPase…….ATP hydrolase

BER……..Base excision repair

BLAST…….Basic local alignment search tool

Cys……Cysteine

dd$H_2O$……..double-distilled water

DDT……..DNA damage tolerance

DMSO……..Dimethyl sulfoxide

DNA…….Deoxyribonucleic acid

E1……..Ub activating enzyme

E2……..Ub conjugation enzyme

E3……..Ub ligase

EDTA……(Ethylenediamine)tetraacetic acid

g…….Gram (unit of mass)

$Gal_{AD}$…….Galactose activating domain

$Gal_{BD}$…….Galactose binding domain

Gly…….Glycine

GST……...Glutathione S-transferase

HCl……....Hydrochloric acid

His…….Histidine

IPTG……..Isopropylthio-β-D-galactoside

L……Litre

LB…….....Luria broth

Leu……Leucine

LiOAc……...Lithium acetate

Lys……Lysine

µL…….....Microlitre

mL……Millilitre

MMR……Mismatch repair

MMS……Methyl methanesulfonate

NER…….....Nucleotide excision repair

ORF…….....Open reading frame

PBS……..Phosphate buffered saline

PBST……...PBS with 0.05% Tween 20 polyoxyethylene 20 sorbitan monolaurate

PCNA……..Proliferating cell nuclear antigen

PCR…….Polymerase chain reaction

PEG…….Polyethylene glycol

Polη……..Polymerase eta

Polζ……..Polymerase zeta

PVDF……...Polyvinylidene diflouride

SD……Synthetic dextrose

SDS……..……...Sodium dodecyl sulfate

SDS-PAGE……..SDS-polyacrylamide gel electrophoresis

SOC…….Super optimal broth with catabolite repression

ssDNA…….Single-stranded DNA

SUMO…….Small Ub related modifier

TAE……Tris-acetate EDTA buffer

TE……Tris EDTA buffer

TEMED……...N,N,N’,N’-Tetramethylethylenediamine

TLS……..Translesion DNA synthesis

Trp……...Tryptophan

UV……...Ultraviolet

Ub……...Ubiquitin

Ubc……..Ub-conjugating enzyme

V……..Volts

v/v……Volume/volume

XP……Xeroderma pigmentosum

XPV……XP variant

YPD……Yeast-extract peptone dextrose

CHAPTER ONE

# DNA DAMAGE TOLERANCE AND THE KNOWN ROLES OF RAD5

## 1.1 DNA Damage Tolerance (DDT) in *Saccharomyces cerevisiae*

*Saccharomyces cerevisiae* utilizes numerous DNA repair mechanisms to maintain the fidelity of the DNA, including base excision repair (BER), nucleotide excision repair (NER), mismatch repair (MMR), homologous recombination (HR) and non-homologous end joining (NHEJ) (Friedberg et al., 2006). Occasionally DNA damage may elude repair by these mechanisms, or may occur during replication, resulting in replication blocking lesions. In order for the cells to maintain genomic stability and viability mechanisms have evolved to tolerate DNA damage separate from repair. These mechanisms of DNA damage tolerance (DDT) are considered to be equally significant to the biology of *S. cerevisiae* as DNA repair mechanisms (Friedberg et al., 2006).

### 1.1.1 Epistasis groups of radiation repair genes in *Saccharomyces cerevisiae*

The yeast genome was initially suggested as a target for radiation sensitivity in 1949 when it was observed that sensitivity to radiation killing was dependent on the state of ploidy in the cells (Laterjet and Ephrussi, 1949). Extensive genetic analysis began in the 1970s following isolation of the first radiation sensitive yeast mutants near the end of the 1960s (Friedberg, 1988; Nakai and Matsumoto, 1967). By the 1980s over 30 yeast genes had been attributed to resistance to killing by UV or ionizing radiation, termed *RAD* (*RAD*iation sensitive) genes (Friedberg, 1988). The *RAD* genes have since been organized into 3 main epistasis groups responsible for mediating different mechanisms of handling DNA damage in *S. cerevisiae*.

An epistatic relationship between two genes is observed when the phenotype of a mutation in one gene overrides the phenotype of a mutation in the other, and indicates that the two genes are involved in sequential steps of a multistep biochemical pathway. The two genes would thus be defined as belonging to the same epistasis group. Alternatively, an additive or synergisitic relationship results when two different mutations affect different biochemical processes, and the genes containing the mutations would be defined as belonging to separate epistasis groups (Friedberg et al., 2006). The three main epistasis groups of *RAD* genes in *S. cerevisiae* are known as the *RAD3*, *RAD52* and *RAD6* groups. Mutations affecting the *RAD52* epistasis group are associated with a high sensitivity to ionizing radiation, and are responsible for mediating HR repair of double strand breaks in the DNA. The *RAD3* group mediates NER and the genes are associated with resistance to UV radiation. Genes that did not fall under the scope of the *RAD3* and *RAD52* groups were historically placed in the *RAD6* epistasis group of radiation repair (Friedberg, 1988; Prakash et al., 1993). The *RAD6* group was thought to mediate a process utilized when the other two repair mechanisms failed and was originally termed post-replication repair (PRR). The genes assigned to each radiation repair epistasis group are listed in Table 1.1.

### 1.1.2 Yeast DNA post-replication repair

Early studies of radiation repair observed that the treatment of yeast cells with UV radiation resulted in transient gaps in the newly synthesized DNA. In a *rad6* mutant the presence of these radiation-induced gaps during replication were prolonged, indicating that the *RAD6* group was involved in a repair process following replication which was thus termed PRR (Prakash, 1981). However, other studies of genes assigned to the *RAD6* epistasis group observed that UV-induced pyrimidine dimers causing single-strand gaps in newly synthesized DNA were

**Table 1.1 - Radiation repair epistasis groups in *S. cerevisiae.***

| RAD3 group | RAD52 group | RAD6 group |
|---|---|---|
| *RAD1* | *RAD50* | *RAD5* (*REV2*) |
| *RAD2* | *RAD51* | *RAD6* |
| *RAD3* | *RAD52* | *RAD18* |
| *RAD4* | *RAD54* | *REV1* |
| *RAD7* | *RAD55* | *REV3* |
| *RAD10* | *RAD56* | *REV7* |
| *RAD14* | *RAD57* | *MMS2* |
| *SSL1* | *RAD59* | *UBC13* |
| *SSL2 (RAD25)* | *XRS2* | |
| *TFB1* | *MRE11* | |
| *RAD16* | | |
| *RAD23* | | |
| *MMS19* | | |

Friedberg *et al*., 2006 and Friedberg *at el*., 1991.

retained after the events of PRR, indicating that the damage was merely bypassed instead of repaired (Bridges and Munson, 1968; Ganesan, 1974). Based on this evidence, PRR has since be re-named DNA damage tolerance (DDT) to better reflect the physiological processes mediated by the *RAD6* epistasis group (Andersen et al., 2008).

### 1.1.3 Identification of error-free and error-prone DDT mechanisms

Since its initial discovery, the process of DDT has been separated into two distinct damage bypass mechanisms, one which acts in an error-prone, or mutagenic, manner while the other utilizes an error-free method. Initial evidence for the error-prone method of DDT arose from the experiments for the initial identification of the genes involved, *REV1*, *REV3* and *REV7*. The *REV* genes were identified as those required for UV induced reversion of the *arg4-17* and *lys1-1* alleles in yeast (Lawrence et al., 1985; Lemontt, 1971), and were subsequently assigned to the *RAD6* epistasis group (Friedberg, 1988). Mutations in these genes result in the loss of the mutagenesis mechanism in *S. cerevisiae*. However, *rad6* and *rad18* mutants have distinctly different phenotypes than *rev* mutants. They are significantly more sensitive to UV radiation, in addition to abolishing UV induced mutagenesis (Prakash et al., 1993). Mutations in *RAD6* and *RAD18* also extend the time required to fill single-strand gaps caused by UV radiation to a much greater extent than a *rev3* mutant (Prakash, 1981). This evidence led to initial speculation that DDT mediates two different mechanisms, one which is error-prone requiring the *REV* genes, and one which is error-free, with *RAD6* and *RAD18* responsible for events upstream of both processes (Prakash et al., 1993).

Apart from *RAD5*, the genes involved in the error-free mechanism of DDT were not identified for several decades after the discovery of DDT. *RAD5* was initially identified as *REV2*

in the same study identifying *REV1* and *REV3* (Lemontt, 1971). However, the effect of a *rad5* mutant on UV induced mutagenesis was later demonstrated to be specific to reversion of only the *arg4-17* allele, and it was determined that *RAD5* was not in general required for the mutagenesis mechanism in yeast. It was subsequently theorized that *RAD5* was most likely involved in the error-free process of DDT (Johnson et al., 1992; Johnson et al., 1994). *MMS2* was initially identified from the *mms2-1* mutant allele isolated based on its enhanced sensitivity to the DNA alkylating agent MMS (Prakash and Prakash, 1977). However, involvement of the gene in the error-free mechanism of DDT was not characterized until 1998, nearly two decades after the proposal of error-free DDT (Broomfield et al., 1998). *MMS2* was demonstrated to have an epistatic relationship with *RAD18* while also being synergistic with *REV3*, indicating its placement in the *RAD6* epistasis group downstream of *RAD6* and *RAD18*, but in a separate biochemical pathway than the *REV* genes. Additionally, the *mms2* mutant also exhibited elevated rates of UV induced mutagenesis, further indicating the requirement of the gene for an error-free mechanism of DNA damage bypass, the loss of which causes all bypass to be routed through the error-prone pathway thus increasing rates of mutagenesis (Broomfield et al., 1998; Xiao et al., 1999). The third member of error-free DDT, *UBC13*, was identified shortly after the characterization of *MMS2* in DDT (Brusky et al., 2000; Hofmann and Pickart, 1999). Classification of *UBC13* into the *RAD6* epistasis group was dependent on the characterization of *MMS2*. *MMS2* encodes a protein similar to a ubiquitin-conjugating (Ubc) enzyme, but lacking the active site Cys residue required for ubiquitination activity, and was proposed to function in complex with a Ubc protein (Broomfield et al., 1998; Xiao et al., 1999). Ubc13 was identified as the Ubc that functioned in complex with Mms2, and was subsequently characterized as a member of error-free DDT by the same methods as *MMS2* (Brusky et al., 2000).

Based on the genetic interactions of the genes assigned to the *RAD6* epistasis group, DDT is considered to consist of a branching pathway. *RAD6* and *RAD18* are involved in the initial steps upstream of the two branches, with *REV1, REV3, REV7* and *RAD30* mediating the error-prone branch, and *RAD5*, *MMS2* and *UBC13* required for the error-free branch (Andersen et al., 2008; Hoege et al., 2002; Prakash et al., 1993; Ulrich, 2011; Zhang et al., 2011) (Figure 1.2).

### 1.1.4 Covalent modification of proliferating cell nuclear antigen (PCNA)

#### 1.1.4.1 Ubiquitin

Ubiquitin (Ub) is a 76 amino acid protein that can be found free or covalently attached to substrate proteins throughout the cell. Covalent attachment of Ub occurs via an enzymatic cascade involving the Ub-activating enzyme (E1), a Ub-conjugating enzyme (E2), and a Ub-ligase (E3) as depicted in Figure 1.1 (Deshaies and Joazeiro, 2009; Hochstrasser, 1996; Welchman et al., 2005). Ubiquitination is highly conserved throughout eukaryotes, and serves as an important signaling mechanism within the cell. The first step of ubiquitin attachment to a substrate requires activation of Ub in an ATP dependent manner by the E1, resulting in attachment of Ub to the active site Cys of the E1 by a thioester bond. The activated Ub molecule is subsequently transferred to the active site Cys residue of the E2. Finally, the E2, with or without the help of a target specific E3, catalyzes the formation of an isopeptide bond between the C-terminal Gly residue of the Ub molecule and the ε-amino group of a Lys residue in the target protein. Target substrates can be ubiquitinated at multiple Lys residues, resulting in a multi-ubiquitinated protein, or a covalently bound Ub molecule may be further modified resulting in poly-Ub chains (Deshaies and Joazeiro, 2009; Welchman et al., 2005). Ub is best known for its signaling role in degradation of target proteins by the 26S proteasome, primarily

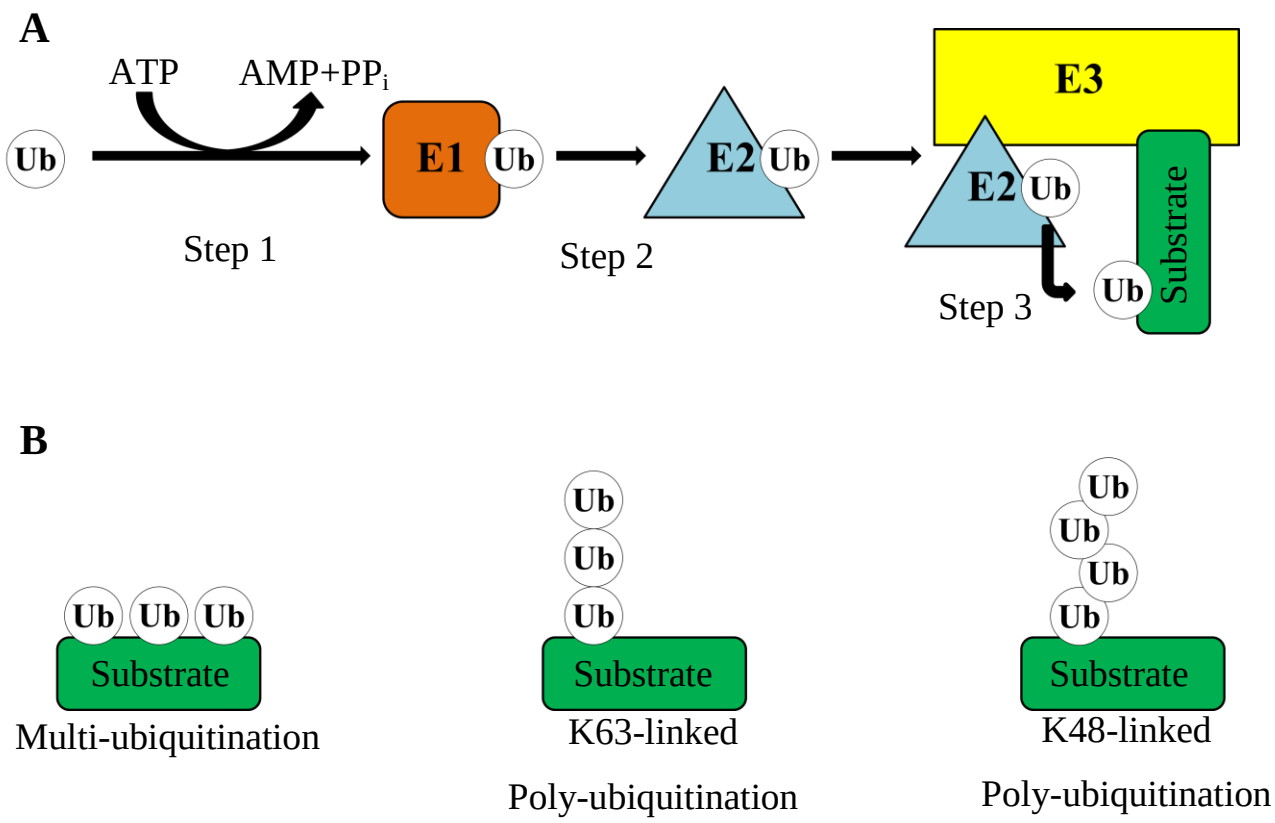


**Figure 1.1. Covalent attachment of ubiquitin to protein substrates.** (**A**) Covalent attachment of Ub molecule to target proteins (ubiquitination) is accomplished through a sequential mechanism. A ubiquitin-activating enzyme (E1) first activates the Ub in and ATP-dependent manner, and the Ub molecule is attached to the active site Cys residue of the E1 by a thioester bond (Step 1). The Ub molecule is subsequently transferred to a ubiquitin-conjugating enzyme (E2), to which it is again bound to an active site Cys via a thioester bond (Step 2). In the final step, the C-terminal Gly residue of Ub is covalently bound to the ε-amino group of a Lys residue in the target protein, with or without the assistance of a ubiquitin ligase (E3) (Step 3). Modification of a protein with a single Ub molecule is termed mono-ubiquitination. (**B**) Additional rounds of ubiquitination at multiple Lys residues of the target protein results in multi-ubiquitination. Ub chains may also be synthesized via the sequencial addition of Ub molecules to the one covalently bound to the substrate protein. Poly-Ub chains are formed in a Lys48-dependent manner, recognized in the cell as a signal for proteosomal degradation, or as non-canonical Lys63-linked chains, a signal for the DNA damage tolerance pathway.

important in the control of short-lived regulatory proteins (Hochstrasser, 1996; Pickart, 1997). Poly-ubiquitin chains can be generated in canonical or non-canonical formats. The canonical poly-Ub chains are formed through linkage of the Ub molecules at the Lys48 residue, while non-canonical poly-Ub chains are linked through Lys63 (Pickart, 2000). Lys48-linked chains are typically recognized by the 26S proteosome and are the most abundant of the poly-Ub chains, while Lys63-linked chains are utilized as a signaling mechanism unrelated to protein degradation in the cell. A study examining the effects of point mutations disrupting the formation of poly-Ub chains in the cell found that a K63R mutant exhibited sensitivity to DNA damaging agents without affecting protein turnover (Spence et al., 1995). This suggested that Lys63-linked poly-Ub chains function in a DNA repair pathway instead of protein degradation. Synthesis of Lys63-linked chains has since been attributed to the Mms2 and Ubc13 protein complex, linking it to DDT (Hofmann and Pickart, 1999; Ulrich, 2003; VanDemark et al., 2001).

#### 1.1.4.2 E2-E3 Complexes in DDT

*RAD6*, the founder of the epistasis group of radiation sensitive genes that mediate DDT, was identified as encoding an E2 enzyme as early as 1987 based on its ability to be isolated by a Ub affinity column (Jentsch et al., 1987). In addition to its role in DDT, Rad6 is also required for sporulation and N-end rule protein degradation in yeast (Andersen et al., 2008; Prakash, 1994). The 172 amino acid protein contains a single Cys residue located at position 88 to serve as the E2 active site nucleophile, and mutation of Cys88 to either Val or Ala abolishes the enzymatic activity and is functionally identical to *rad6Δ*. *RAD18* encodes an E3 (Ub-ligase) enzyme that belongs to the RING finger family of E3s which forms a stable heterodimer with Rad6, suggesting that Rad6 and Rad18 function together as an E2:E3 complex with Rad18 providing a context for functional specificity to DDT (Bailly et al., 1994; Lorick et al., 1999;

Saurin et al., 1996). Rad18 also exhibits an ssDNA binding activity which likely targets the Rad6-Rad18 complex to sites of replication blocking damage in the DNA (Bailly et al., 1997).

Rad6 and Rad18 do not form the only E2-E3 complex involved in DDT. Mms2 and Ubc13 function as a heterodimeric E2 in the *in vitro* synthesis of Lys63-linked poly-Ub chains (Hofmann and Pickart, 1999). The error-free DDT gene, *RAD5*, in turn encodes another RING finger E3, which physically interacts with both Rad18 and Ubc13 (Lorick et al., 1999; Saurin et al., 1996; Ulrich and Jentsch, 2000). Thus Rad5, Ubc13 and Mms2 form a second E2-E3 complex involved in DDT, and Rad5 is thought to target the E2 activity of Mms2-Ubc13 to sites of DNA damage via its interaction with Rad18.

#### 1.1.4.3 Ubiquitination of PCNA

Characterization of the two E2-E3 complexes functioning in the processes of DDT, both upstream of the branch between the error-prone and error-free mechanisms, and involved specifically in the error-free mechanism, indicated that some target protein(s) must be ubiquitinated as part of the physiological processes of DDT. However, that target substrate was not apparent until 2002 when proliferating cell nuclear antigen (PCNA), the replicative sliding clamp, was revealed as a substrate for covalent attachment of at least two Ub molecules at its Lys164 residue upon DNA damage in the cell (Hoege et al., 2002). The first suggestion that PCNA, encoded by *POL30* in yeast, was involved in DDT arose with the discovery of a UV sensitive allele of the gene, *pol30-46*, that shared an epistatic relationship with *RAD6* and *RAD18* (Torres-Ramos et al., 1996). Identification of PCNA as a substrate for ubiquitination provided the details of its physiological role in DDT that genetic evidence could not provide. Attachment of the first Ub to PCNA is mediated by Rad6 and Rad18, while attachment of the second Ub is

carried out by Rad5, Mms2 and Ubc13. With this data a functional model of DDT could finally be proposed where post-translational modification of PCNA determines the activation of the cellular function. Mono-ubiquitination of PCNA by the Rad6-Rad18 heterodimer activates DDT in general, at which point either branch of the pathway can be activated. Either the error-prone components are recruited, or the protein complex of Rad5-Ubc13-Mms2 can subsequently attach a Lys63-linked poly-Ub chain to activate the error-free mechanism of DDT (Hoege et al., 2002). A general model of DDT is depicted in Figure 1.2.

#### 1.1.4.4 Sumoylation of PCNA

While PCNA is a substrate for covalent attachment of Ub, it is also covalently modified by a SUMO molecule in the absence of DNA damage (Hoege et al., 2002). SUMO is a small ubiquitin-related modifier that is covalently bound to target proteins in an enzymatic cascade identical to Ub (Schwartz and Hochstrasser, 2003). The SUMO molecule is first activated by a SUMO-activating enzyme (E1), then transferred to a SUMO-conjugating enzyme (E2), and is finally covalently bound to the ε-amino group of a Lys residue in the target protein, often with the assistance of a SUMO-ligase (E3) (Gareau and Lima, 2010). Interestingly, PCNA is modified by both SUMO and Ub at the Lys164 residue (Hoege et al., 2002). Ubc9 and Siz1 function as the E2 and E3, respectively, for sumoylation of PCNA in *S. cerevisiae* (Gareau and Lima, 2010; Johnson and Blobel, 1997; Stelter and Ulrich, 2003). It is now understood that SUMO is required for the recruitment of Srs2 to the replication fork, where it prevents undesired activation of HR by directly interfering with the formation of Rad51-ssDNA filaments (Krejci et al., 2003; Pfander et al., 2005; Veaute et al., 2003). If Srs2 cannot be recruited to the replication fork and a replication blocking lesion is encountered, HR can be activated by the exposure of ssDNA and subsequently prevent the activation of DDT.

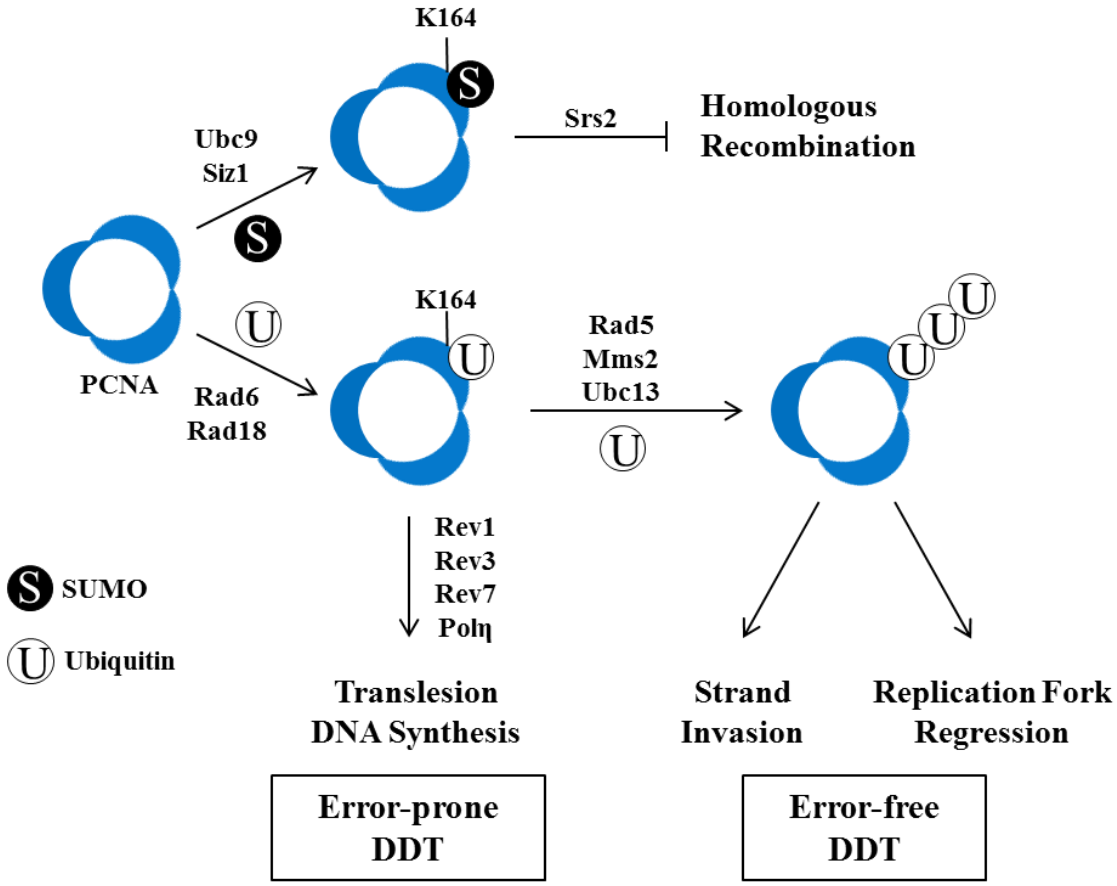


**Figure 1.2 - Schematic diagram of the current working model for DNA damage tolerance**. DNA damage tolerance (DDT) is activated upon mono-ubiquitination of the K164 residue of at least one monomer of PCNA, the homotrimeric replicative sliding clamp, by the Rad6-Rad18 E2-E3 complex at sites of stalled replication caused by lesions in the DNA. Subsequently, specific error-prone translesion DNA polymerases may be recruited to the damage site to directly replicate past the lesion. Alternatively, a heterodimeric E2, Mms2-Ubc13, with the assistance of the Rad5 E3 can further modify PCNA with K63-linked poly-Ub chains. Poly-ubiquitination of PCNA activates the error-free pathway of DDT. Error-free DDT utilizes a template switch thought to be mediated a replication fork regression mechanism or a strand invasion mechanism involving components of the HR machinery. PCNA is also modified through covalent attachment of SUMO to the K164 residue by Ubc9 and Siz1, a SUMO E2 and E3, respectively. SUMO modified PCNA recruits Srs2 to the replication fork, and Srs2 prevents undesired activation of HR by inhibiting the formation of Rad51-ssDNA nucleoprotein filaments. In the absence of Srs2, HR inhibits activation of DDT.

### 1.1.5 Translesion DNA synthesis (TLS)

Covalent modification of PCNA plays a vital role in coordinating the error-free and error-prone mechanisms of DDT in yeast. Mono-ubiquitination of PCNA by Rad6 and Rad18 mediates activation of the mutagenic pathway, while further poly-ubiquitination of the already modified PCNA activates the error-free pathway. The error-prone pathway of DDT was initially defined by its association with UV induced mutagenesis in yeast (Lemontt, 1971; Prakash, 1981). The mechanisms of this mutagenic pathway have since been well defined, with specialized error-prone DNA polymerases replicating directly past lesions in the DNA (Prakash et al., 2005). This process is termed translesion DNA synthesis (TLS). Specifically, TLS bypass is mediated by the Y family of DNA polymerases Rev1 and Polη, and Polζ, which belongs to the B family of polymerases that also includes the replicative polymerases. All three TLS enzymes lack the 3'-5' proofreading exonucleases activity of the replicative polymerases, a property which imparts a relaxed fidelity for nucleotide incorporation resulting in a highly mutagenic bypass mechanism.

*REV1* encodes an enzyme with deoxycytidyl transferase activity, catalyzing insertion of dCMP opposite lesions in the DNA, and as such Rev1 is not precisely a DNA polymerase in the same sense as other DNA polymerases (Nelson et al., 1996; Prakash et al., 2005). The biochemical activity of Rev1 is actually fairly weak compared to other polymerases, and its most important function appears to be as a structural element for the recruitment of the other TLS polymerases. Consistently, Rev1 contains PCNA and Ub-binding domains, and physically interacts with Polζ and Polη independently of its transferase activity (Sale et al., 2012).

Polη, encoded by the *RAD30* gene in *S. cerevisiae*, was the last member of the TLS polymerases to be identified (McDonald et al., 1997). Polη is uniquely adapted for the correct insertion of AA opposite UV induced *cis-syn* TT dimers in the template DNA, and the structure of the active site prevents distortion of the DNA by the *cis-syn* TT dimers maintaining the correct reading frame (Johnson et al., 1999; Masutani et al., 1999; Prakash et al., 2005). The ability of Polη to correctly replicate past *cis-syn* TT dimers imparts a relatively error-free activity to the polymerase, particularly compared to the other TLS enzymes. The polymerase is extremely inefficient at replication past other forms of DNA damage, and is primarily favoured for bypass of *cis-syn* TT dimers.

Polζ is formed by the association of Rev3 and Rev7 as a functional heterodimer (Prakash et al., 2005). *REV3* encodes the catalytic subunit of the polymerase, while *REV7* encodes the regulatory subunit which physically interacts with Rev1. Polζ is relatively inefficient at insertion directly across from DNA lesions, but it is uniquely efficient at extending from mismatched primers, even when lesions distort the structure of the DNA (Johnson et al., 2000). This unique property of Polζ at the extension step of DNA replication leads to a model where either Rev1 or Polη inserts nucleotides directly opposite sites of DNA damage, and Polζ carries out extension to a point where the regular replicative polymerases can resume function (Prakash and Prakash, 2002).

### 1.1.6 Error-free DDT

#### 1.1.6.1 Identification of the known components of DDT

While the molecular mechanisms utilized by the TLS pathway of DDT are relatively well characterized, the downstream events of error-free DDT are largely speculation. Genetic

evidence in yeast indicates that the error-free branch of DDT likely comstitutes the preferred mechanism, as mutations in the error-free pathway confer a greater sensitivity to DNA damaging agents than mutations disrupting TLS (Brusky et al., 2000; Xiao et al., 1999). Initial evidence for error-free DDT was based on the distinct differences between the *rev* mutants and the *rad6* and *rad18* mutants. The *rad6* and *rad18* mutants are extremely sensitive to killing by DNA damaging agents, while the *rev* mutants are relatively resistant in comparison (Xiao et al., 1999). *RAD5* was thought to potentially be involved in an error-free mechanism, but its phenotypes were complicated. There was initial evidence of its involvement in mutagenesis, which was later refuted, and its sensitivity to DNA damaging agents was somewhere in between the sensitivity of the *rad6* and *rad18* mutants and the *rev* mutants (Johnson et al., 1992; Lemontt, 1971). Strong evidence for the error-free pathway did not emerge until the characterization of *MMS2* and *UBC13*. Both *mms2* and *ubc13* mutants exhibited a synergistic relationship with *rev* mutants, and display elevated rates of spontaneous mutagenesis (Broomfield et al., 1998; Brusky et al., 2000). However, Rad5, Ubc13 and Mms2 are involved in regulation of the error-free pathway of DDT, but their function has not been able to shed light on the molecular mechanisms employed by the pathway (Hoege et al., 2002; Ulrich and Jentsch, 2000). Two distinct models have been proposed to explain a template switch that would allow error-free bypass of DNA lesions. One model proposes a mechanism utilizing replication fork regression and is also referred to as a chicken-foot model. The other model proposes the recruitment of factors otherwise involved in HR to mediate strand invasion to facilitate the template switch (Broomfield et al., 2001) (Figure 1.3).

#### 1.1.6.2 Strand invasion model

The strand exchange model of error-free DDT details a template switch mechanism that utilizes homologous recombination to pair nascent strands of DNA for continued synthesis of the otherwise blocked strand. This model proposes that subsequent to poly-ubiquitination of PCNA components of the HR system in budding yeast are recruited to the site of damage. According to the model, activation of error-free DDT results in strand invasion, presumably mediated by Rad51, to pair the blocked nascent strand with the opposite newly synthesized nascent strand. Pairing of the strands provides an accurate template for continued synthesis of the blocked strand past the point of damage in its parental template. Finally, the nascent strands are recombined with the parental strands and DNA synthesis is allowed to continue normally. The process of recombination utilized by this template switch mechanism would invariably result in the formation of double Holliday junctions, which the Sgs1 helicase and topoisomerase 3 (Top3) would be needed to resolve (Ball, 2011; Ball et al., 2009). Figure 1.3B depicts the strand exchange model.

A study of the genes required for replication of dsDNA plasmids containing (6-4) photoproducts in one strand opposite C-C in the sister strand in an NER deficient background indicated that both *RAD18* and *RAD52* were required for the majority of successful plasmid replication events, indicating cooperation between HR and DDT (Zhang and Lawrence, 2005). The strand exchange model for the error-free mechanism of DDT would dictate the formation of X-DNA structures during resolution of the double Holliday junctions. Consistent with this model, loss of either *RAD18* or *RAD5* negatively impacts the accumulation of X-DNA structures after treatment of a *top3* null mutant with a DNA damaging agent (Branzei et al., 2008). Additional physical studies have demonstrated that Rad5 can mediate the formation of Holliday junctions containing X-DNA structures in a manner dependent on both of the E3 and ATPase

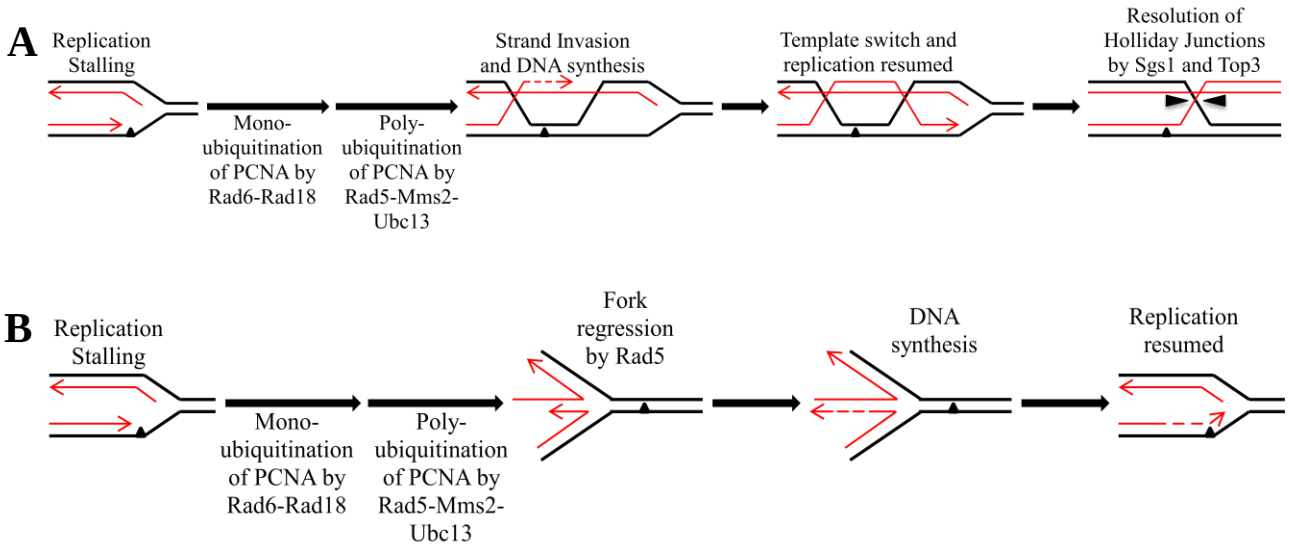


**Figure 1.3 - Proposed mechanisms mediating the template switch during error-free DNA damage tolerance**. (**A**) Stalling of leading strand replication due to damaged DNA in the template strand (▲) creates limited ssDNA, leading to the recruitment of Rad6-Rad18 for the activation of DDT via mono-ubiquitination of PCNA. Sequentially, Rad5-Ubc13-Mms2 poly-ubiquitinate PCNA to activate the error-free branch of DDT. Homologous recombination proteins mediate strand invasion, presumably through the formation of Rad51-ssDNA nucleoprotein filaments, to pair the nascent strands and provide an accurate template for the blocked strand. The blocked leading strand can then be replicated past the damaged site in the parental strand. The leading strand is switched back to its original template, Sgs1 and Top3 resolve the double Holliday junctions, and normal replication is resumed. (**B**) Activation of the error-free branch of DDT occurs as above, but by this model Rad5 is able to carry out replication fork regression. The helicase activity of Rad5 concertedly unwinds and anneals the nascent strands resulting in a chicken foot structure. Replication of the stalled strand can be continued using the newly synthesized sister chromatid past the location of the lesion in the template DNA. Fork regression can then be reversed and normal DNA replication resumed.

activities of the protein (Minca and Kowalski, 2010). A recent screen for genes sharing a synergistic relationship with TLS mutants, presumably indicating a role in the error-free branch of DDT, pulled out the four HR related genes encoding the components of the Shu complex (Ball, 2011; Ball et al., 2009; Bernstein et al., 2011; Mankouri et al., 2007; Xiao et al., 1999). Mutations disrupting several of the key HR genes are now understood to also share a synergistic effect on the sensitivity of cells to killing by DNA damaging agents when combined with mutations in the genes required for TLS, a characteristic genetic relationship observed when two mutations separately disrupt the two mechanisms of DDT. Also *mms2Δ* appears to be epistatic to *sgs1Δ*, the helicase required for resolution of Holliday junctions during HR, indicating *MMS2* acts directly upstream in the same biochemical pathway as *SGS1* (Ball, 2011; Ball et al., 2009). In all, both physical and genetic evidence has been mounting to support an HR mediated strand exchange mechanism employed by error-free DDT.

#### 1.1.6.3 Replication fork regression model

DDT is thought to occur during normal DNA synthesis when the replication fork encounters a lesion which stalls the replication fork machinery. Leading and lagging strand synthesis become uncoupled and ssDNA is exposed. Rad18 is recruited via its affinity for ssDNA, bringing Rad6 with it. Together Rad6 and Rad18 attach a single ubiquitin monomer to the Lys164 residue of PCNA, at which point the TLS enzymes or Rad5 can be subsequently recruited. When error-free DDT is to be activated Rad5 is recruited to the stalled replication fork likely based on its ability to bind PCNA and Rad18. Rad5 physically interacts with Ubc13, bringing in the Ubc13-Mms2 E2 heterodimer in turn, targeting them for covalent attachment of a Lys63-linked Ub chain to the already modified PCNA. Upon poly-ubiquitination of PCNA a

template switch mechanism is employed to ensure replication past the damaged DNA utilizing an undamaged template (Zhang and Lawrence, 2005).

The replication fork regression model of error-free DDT posits that Rad5 once recruited to the site of DNA damage carries out the replication fork regression, unwinding the parental and nascent strands and annealing both nascent strands together in a chicken foot structure. This provides an undamaged template for continued synthesis of the blocked nascent strand from its sister chromatid in an error-free manner. Once synthesis has bypassed the damaged site in the parental strand Rad5 reverses the replication fork regression by unwinding the nascent strands and re-annealing the nascent strand to the parental strands. This manner of DNA damage bypass would be most important for leading strand synthesis as Okazaki fragments could be utilized to facilitate bypass of damage during lagging strand synthesis (Blastyak et al., 2007). The replication fork regression model of error-free DDT is depicted in Figure 1.3A.

The model for replication fork regression mediating the error-free mechanism of DDT is contingent on the characteristics of the multifunctional Rad5 protein. Specifically, it depends on the putative helicase activity of the 7 conserved domains characteristic of a SWI2/SNF2 helicase/ATPase (Johnson et al., 1992). The SWI2/SNF2 domains characterize a subgroup of the helicase Superfamily 2 which contains a helicases typically involved in chromatin remodeling (Tang et al., 2010). While the SWI2/SNF2 domain of Rad5 possesses DNA dependent ATPase activity, an associated helicase activity is not as certain (Gangavarapu et al., 2006; Johnson et al., 1994). A single study has examined the potential helicase activity if Rad5 *in vitro* (Blastyak et al., 2007). Utilizing model replication fork structures intended to mimic stalled leading strand synthesis and 4 way junctions (such as the chicken foot), Rad5 was shown to unwind the DNA structures it would be required to process according to the fork regression model in an ATP

dependent manner. The experiments revealed that Rad5 facilitated unwinding and annealing in a concerted manner, without exposure of any ssDNA. However, the experiments involved were purely *in vitro* and *in vivo* studies still need to be performed in order to verify the activity and the likelihood of the replication fork regression model of the template switch required for error-free DDT. The replication fork regression model of error-free DDT also fails to explain the requirement of PCNA poly-ubiquitination in the activation of the pathway. It is possible that poly-ubiquitination may serve to inhibit the association of unwanted factors at the site of the DNA damage that might otherwise inhibit replication fork regression, such as the TLS polymerases. The helicase activity of Rad5 would require strict regulation in order to prevent interference with normal DNA synthesis. However, the presence of Rad18 and PCNA mono-ubiquitination is likely required for full recruitment of Rad5 to the replication fork, providing regulation of its activities.

The two proposed mechanisms for mediating the strand exchange during error-free DNA damage bypass are not necessarily mutually exclusive. It is conceivable that the two processes merely represent parallel pathways. The significance of poly-ubiquitination and the exact downstream series of events are not yet understood, and future discoveries in this area should shed light on which method is utilized by the cell, and the conditions dictating activation of the error-free pathway of DDT. Alternatively, replication fork regression via Rad5 may occur prior to strand invasion as part of a mechanism combining the two proposed models. It should be noted that PCNA is constitutively SUMOylated, inhibiting undesirable HR events, and if HR is utilized during error-free damage bypass the inhibition of recombination must first be counteracted (Hoege et al., 2002).

## 1.2 DDT and Cancer

DNA damage tolerance is an important cellular process for the maintenance of genomic stability conserved from yeast to humans (Ulrich, 2011). Due to this conservation, the parallel branches of DDT, one error-free and one mutagenic, have important implications in the development of cancer in humans. Homologues for each of the primary components of DDT in *S. cerevisiae* have been identified in mammalian cells, although multiple homologues exist for the yeast Rad6, and Rad5, and mammals have 2 additional TLS polymerases, Polι and Polκ (Koken et al., 1991; Prakash et al., 2005; Unk et al., 2008; Unk et al., 2006). Since DDT is highly conserved between humans and yeast, *S. cerevisiae* can serve as an important model organism to understand under which situations the different mechanisms of DDT are utilized and how that pertains to the potential development of mutations in humans. One important difference between DDT in humans and budding yeast is reflected in the favoured pathways of DDT. Evidence suggests that the error-free pathway is the preferred branch in yeast, while the mutagenic process of TLS appears to be preferred in mammalian cells (Prakash et al., 2005). To underscore the importance of DDT in the development of cancers in humans, mutations in the XPV/*POLH* gene, encoding Polη in humans, results in xeroderma pigmentosum variant (XPV), a modified form of XP (Masutani et al., 1999). XPV is linked to hypersensitivity to UV damage and predisposition to cancer.

### 1.3 Structure and Functions of Yeast Rad5

Rad5 remains an interesting component of DDT despite being first identified as *REV2* in 1971 and initial characterization of the gene and protein in the early 1990s (Johnson et al., 1992; Johnson et al., 1994; Lemontt, 1971). *RAD5* encodes a 134 kDa protein, 1169 amino acids in length (Johnson et al., 1992). Initial sequence analysis of Rad5 revealed the 7 conserved domains of SWI2/SNF2 helicase comprising the majority of the C-terminal half of the protein, a

leucine heptad repeat from residues 323 to 338, and a putative zinc finger from residues 914 to 960 embedded within the SWI2/SNF2 domain (Johnson et al., 1992). Identification of the RING finger family of E3 enzymes led to reclassification of the putative zinc finger as a conserved RING finger domain (Lorick et al., 1999). Most recently a conserved domain in the N-terminal regions of SWI2/SNF2 proteins typified by HIP116 and Rad5 was identified, and is termed the HIRAN domain (Iyer et al., 2006). The known domains of Rad5 are depicted schematically in Figure 1.4.

Functional studies of Rad5 have associated a DNA dependent ATPase activity with the SWI2/SNF2 domain, although data conflicts as to whether it is dependent on ssDNA or specific DNA structures (Blastyak et al., 2007; Johnson et al., 1994). A DNA helicase activity has also been attributed to the SWI2/SNF2 domain of Rad5, but the physiological significance is not yet fully understood (Blastyak et al., 2007). The RING finger of Rad5 imparts and E3 activity to facilitate poly-ubiquitination of PCNA and activation of the error-free branch of DDT. The RING finger is required for targeting the Ubc13-Mms2 heterodimer to PCNA, and enhances the synthesis of Lys63-linked poly-Ub chains by the E2 (Parker and Ulrich, 2009). Point mutations disrupting the ATPase and E3 activities of Rad5, D681A,E682A and I916A respectively, have been critical to the functional analysis of Rad5, and have been utilized to verify that both activities are required for error-free DDT (Gangavarapu et al., 2006). Both point mutations result in a sensitivity to DNA damaging agents similar to a *ubc13* or *mms2* null mutation (unpublished data) and increase the rates of spontaneous mutagenesis similar to the other mutations abolishing error-free DDT (Gangavarapu et al., 2006). No specific functions have been assigned to either the HIRAN domain or the leucine heptad repeat (Iyer et al., 2006).

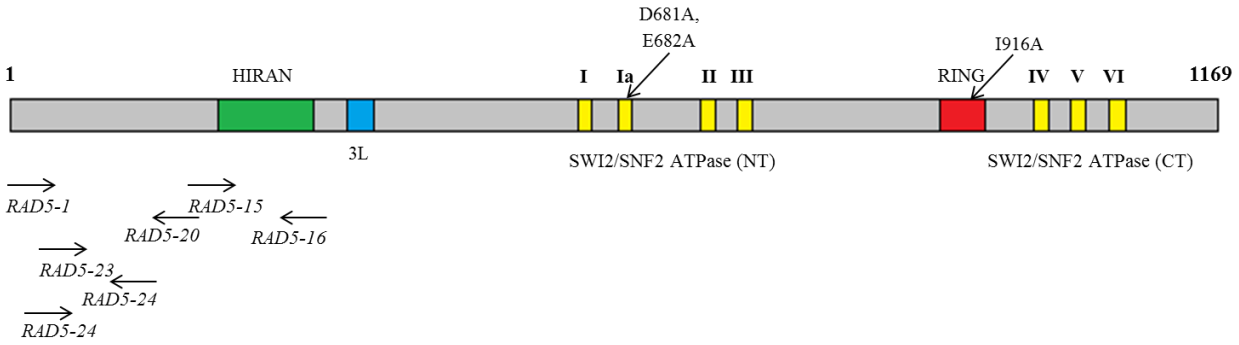


**Figure 1.4. Model of the Rad5 protein indicating the relative positions of the known domains**. *RAD5* encodes a multifunctional 134 kD protein 1169 amino acids in length. The protein contains a HIRAN domain, indicated in green and by HIRAN above, from residues 171-286, identified based solely on the conservation of the amino acid sequence amongst several SWI2/SNF2 family proteins. Adjacent to the HIRAN domain is a leucine heptad repeat or leucine zipper (3L, blue) from residues 323-338. The leucine heptad repeat contains 3 Leu residues, each separated by 6 amino acids, and is preceeded by a basic region in the protein. Both the leucine heptad repeat and HIRAN domain of Rad5 have been theorized to play a role in DNA binding, but no activities have yet been functionally demonstrated for either region. The C-terminal half of the protein contains the 7 conserved domains of a SWI2/SNF2 ATPase, indicated in yellow and labeled as N-terminal (NT) or C-terminal (CT). The domain locations by number of amino acids are as follows: I, 529-540; Ia, 589-605; II, 678-687; III, 706-713; IV, 1016-1033; V, 1072-1095; VI, 1109-1116. The SWI2/SNF2 domains are associated with a DNA dependent ATPase activity of Rad5. Lastly, the Rad5 protein contains the RING finger (indicated in red and labeled as RING) characteristic of the RING finger family of E3 enzymes, comprised of amino acids 914-960. Rad5 functions as an E3 enzyme to the Mms2-Ubc13 E2 heterodimer for poly-ubiquitination of PCNA, for which the RING finger is required. Both the ATPase and E3 enzyme activities are required for functional error-free DDT. Point mutations utilized to disrupt the ATPase and E3 activities of the protein are indicated by arrows and the amino acid changes indicated. Horizontal arrows below the diagram indicate the primers and their positions utilized in the construction of Rad5 truncations employed in this study.

While some activities of Rad5 have been well characterized, there remains evidence that not all activities of this multifunctional protein have been discovered. Notably, the phenotypes of the *rad5* null mutant set it apart from the *mms2* and *ubc13* null mutants. Specifically, the *rad5* null mutant is significantly more sensitive to killing by DNA damaging agents than either *mms2Δ* or *ubc13Δ*, but not as sensitive as a *rad18* null mutant (Brusky et al., 2000; Hoege et al., 2002). This phenotype provides a clear difference between Rad5 and the other members of error-free DDT, suggesting an additional role for Rad5 in the DNA damage response of yeast cells. Additionally, the point mutations abolishing the ATPase and ubiquitin ligase activities of Rad5 are not as sensitive to killing as the *rad5* null mutant, but instead closely resemble the *ubc13* and *mms2* null mutants (unpublished data). The sensitivity of the various *rad5* mutations to killing by DNA damaging agents compared to other DDT mutants clearly suggests that Rad5 carries out additional functions outside of the error-free branch of DDT.

The conserved SWI2/SNF2 ATPase domain of Rad5 may provide some clue to the uncharacterized role(s) of Rad5 within the cell. The SWI2/SNF2 domain is characteristic of a subgroup of the Superfamily 2 of helicases (Tang et al., 2010). The domain is named for Swi2, and ATPase that functions in the SWI/SNF chromatin remodeling complex in *S. cerevisiae*. Interestingly, both NER and HR repair include a protein containing the SWI2/SNF2 domain, Rad16 and Rad54, respectively (Eisen et al., 1995). Rad16 acts as a helicase to remodel the chromatin to facilitate the repair process, and Rad54 possesses a processive motor activity allowing translocation along DNA supportive of a role in chromatin remodeling as part of HR repair (Ceballos and Heyer, 2011; Yu et al., 2011). Rad5 may serve a similar function to facilitate the mechanisms of DNA damage bypass utilized by DDT. However, the genetic data regarding the ATPase mutant of Rad5 suggests that the ATPase activity is only important for the

error-free branch of DDT. Therefore a chromatin remodeling activity is unlikely to explain greater sensitivity of the *rad5* null mutant to DNA damaging agents compared to other error-free DDT mutants.

The initial identification of *RAD5* as *REV2*, a gene required for UV induced mutagenesis in yeast (Lemontt, 1971), may point to an alternative possibility for the unknown functions of the protein. Initial screens identifying the *REV* genes were based on their requirement for UV induced reversion of the *arg4-17* and *lys1-1* alleles, and those genes are now known to encode TLS enzymes (Lemontt, 1971; Prakash et al., 2005). Subsequent analysis of *rad5Δ* revealed that the gene was not in fact required for most UV induced mutagenesis, and is only partially required for UV induced reversion of the *arg4-17* allele unlike the TLS genes (Johnson et al., 1992). However, this phenotype may actually indicate a partial role for TLS. Sequence analysis of the *arg4-17* allele indicates that reversion is predominantly due to a T to C transition of T127 likely as a result of insertion of a G opposite a (6-4) TT photoproduct, suggesting a role for Rad5 in TLS bypass of (6-4) TT photoproducts (Gangavarapu et al., 2006; Zhang and Siede, 2002). More recent data indicates that Rad5 is also required for Polζ mediated TLS bypass of abasic sites and G-AAF adducts (Gangavarapu et al., 2006; Pages et al., 2008). Interaction data indicates that Rad5 does not interact with either Rev3 or Rev7, the subunits of Polζ, and instead physically binds Rev1 (Pages et al., 2008). Together, the data suggests that Rad5 functions partially in TLS, and that its role in TLS is mediated via a physical interaction with Rev1, an important scaffolding protein for assembly of TLS proteins at sites of DNA damage.

While there is mounting evidence for additional roles for Rad5 within DDT apart from its ATPase and E3 activities in the error-free branch, the unique phenotypes of a *rad5* null mutant may also be explained by a function outside of DDT altogether.

## 1.4 Rationale for This Study

DNA damage tolerance is an important mechanism that serves to prevent replication fork collapse and maintain genomic stability in *S. cerevisiae*. DDT facilitates bypass of replication blocking lesions in the DNA utilizing both mutagenic and error-free mechanisms. These mechanisms are evolutionarily conserved in mammalian cells, and have implications in the development of cancers in humans. While many of the details of the molecular mechanisms involved have been elucidated, a number of details remain unclear. The Rad5 protein provides a particular mystery as to its function in DDT. ATPase and ubiquitin ligase activities of the protein have been associated with the error-free pathway of DDT. However, there is significant evidence for additional functions of the protein (Gangavarapu et al., 2006; Hoege et al., 2002; Pages et al., 2008). Most notably, the *rad5* null mutant is significantly more sensitive to killing by DNA damaging agents than other mutants disrupting the error-free pathway of DDT. The objective of this research was to better understand what roles Rad5 may be playing outside of its function in error-free DDT.

Rad5 functions partially in TLS bypass of DNA lesions, although its exact role is not understood. Rad5 does physically bind the Rev1 protein, a TLS enzyme and scaffolding protein for the assembly of the other TLS polymerases, and this interaction likely mediates the TLS activity of Rad5. We set out to target this physical interaction to elucidate the role of Rad5 in TLS. If the interaction can be abolished without disrupting the other functions of Rad5, it will provide the framework for genetic and physical studies of the TLS activity of Rad5. To this end we designed a series of sequential truncations of Rad5 in an attempt to identify the key region for the interaction with Rev1. The yeast two-hybrid assay was utilized to assess the interaction between Rad5 and Rev1, and the results are presented here along with discussion of the next

steps in identifying the key residues in Rad5 for maintaining the interaction. Design of a TLS deficient *rad5* mutant and the subsequent experiments are explored.

While Rad5 possesses at least one uncharacterized function in the TLS pathway of DDT, the unique phenotype of the *rad5* null mutant may also be explained by the protein functioning in a different cellular process altogether. Epistasis analysis of the sensitivity of mutants of various upstream DDT mutants in combination with *rad5* null mutant is carried out here to determine whether *RAD5* has a hypostatic or additive relationship with these upstream DDT genes. The results and the implications on the current working model of DDT are explored further in the discussion. It is our hope that the findings here will provide future insight into the mechanisms of DDT, particularly how the cell chooses between the error-free and mutagenic pathways. Conservation of DDT in humans means that this insight will further our understanding of one route through which mutations, and potentially cancers, can arise in humans.

# CHAPTER TWO

# MATERIALS AND METHODS

## 2.1 Molecular Biology Techniques

### 2.1.1 Plasmid DNA isolation

#### 2.1.1.1 Plasmid isolation by Quantum Prep® kit

Plasmid DNA isolation was primarily performed using the Quantum Prep® Plasmid Miniprep kit purchased from Bio-Rad (Catalogue #732-6100) via the protocol provided with a minor modification. The final step was repeated, resulting in resuspension of the plasmid DNA in 200 μL of sterile dd$H_2O$ (double-distilled reverse osmosized $H_2O$) instead of 100 μL.

#### 2.1.1.2 The boiling method

The boiling method of plasmid preparation was carried out as previously described (Maniatas *et al*., 1982). Bacterial cells were grown overnight at 37°C in 1.5 mL Luria Broth (LB) media (US Biological L1505) (10 g Tryptone, 5 g yeast extract, 5 g NaCl in a total of 1 L dd$H_2O$) with the appropriate drug for selection of the respective plasmids. Cell pellets were collected by centrifugation and resuspended in 350 μL of STET (0.1 M NaCl, 10 mM Tris-HCl pH 8.0, 1 mM (ethylenedinitrilo)tetraacetic acid (EDTA. EMD Chemicals, EX0539-1) pH 8.0, 5 % Triton X-100). 20 μL of lysozyme (10 mg/mL, Sigma L-6876) was added to the Eppendorf tube of resuspended cells, which was mixed gently by inverting the tube 2-3 times, and boiled for 1 minute. Cells were centrifuged at top speed (15,000 rpm) for 10 minutes, and the resultant pellet was removed manually with a toothpick. Two volumes of cold 95% ethanol (approximately 760 μL) and 8 μL were added to the supernatant, and DNA was precipitated at -

20 °C for a minimum of 30 minutes. Samples were centrifuged at top speed for 15 minutes, the supernatant poured off and the pellet allowed to dry completely before being resuspended in 30 µL sterile $ddH_2O$ and stored and -20 °C.

### 2.1.2 Polymerase chain reaction

The protocol for Platinum® *Taq* DNA polymerase purchased from Invitrogen (Carlsbad CA., USA Cat. No. 10966-034) was used as the basis for all PCR performed. The typical PCR reaction mixture was composed as follows: 5 µL of 50 mM 10x PCR buffer (supplied with the purchased Platinum® *Taq*), 1.0 µL of 50 mM $MgCL_2$, 1.8 µL of 2.5 mM dNTPs (prepared from a 100 mM dNTP set, Invitrogen, Cat. No. 10297-018), 0.5 µL Platinum® *Taq* DNA polymerase, 0.5 µL of each primer, 1 µL of appropriate template DNA, brought up to a total volume of 50 µL with sterile $ddH_2O$. A standard PCR cycle was set up as follows: initial denaturation at 94 °C for 2 minutes, denature for 30 seconds at 94 °C, annealing at 55 °C for 30 seconds, extension at 72 °C for 1 minute/kb of the DNA fragment to be amplified, and a final extension of 10 minutes at 72 °C followed by a final holding temperature of 4 °C until samples were removed. The denaturation, annealing and extension cycle was repeated 30 times, and PCR prepared samples were stored at -20 °C until use. All PCR amplified fragments were analyzed by agarose gel electrophoresis prior to use. Oligonucleotides were ordered from Integrated DNA technologies and were specific for each run. All oligonucleotides used in this study are listed in Table 2.1 and their locations relative to the protein are indicated as horizontal arrows in Figure 1.4. Odd numbered labels indicate forward primers, while even numbered labels indicate reverse primers

**Table 2.1 - Oligonucleotides utilized in this study.**

| Oligonucleotide | Sequence (5' – 3') |
|---|---|
| *RAD5-1* | CCG GAT CCA TGA GTC ATA TTG AAC AGG |
| *RAD5-15* | CCC GGA TCC CAG AAA CCA AAC ACG ATT AG |
| *RAD5-16* | CCC GTC GAC TTA ACG TTC CTC AAA AAT GAG AG |
| *RAD5-20* | CCC GTC GAC TTA CGT GTT TGG TTT CTG AAC C |
| *RAD5-23* | CTG GGA TCC GTG AGT GAT ACA ACA GAA GG |
| *RAD5-24* | CTG GTC GAC TTA CGG GGA AGA CGG TAT TTT |
| *RAD5-25* | CTG GGA TCC CCA GAA ATG CCA AAG GAT C |

### 2.1.3 Agarose gel electrophoresis and DNA fragment isolation

DNA samples (plasmid and genomic) were analyzed by agarose gel electrophoresis. Agarose gels were typically made at 0.75 % in 1x TAE (Tris-acetate EDTA), prepared from 50x stock (2.42 g Tris base, 57.1 mL glacial acetic acid, 150 mL EDTA pH 8.0 in a total volume of 1 L diluted in dd$H_2O$). Gels were electrophoresed at 88 V and stained with ethidium bromide for visualization of the DNA. Purification of DNA from an agarose gel was performed by cutting out the appropriately sized band, placing it into a 0.5 mL microcentrifuge tube atop a small amount of cheesecloth, and freezing the sample at -70 °C for a minimum of 20 minutes. The sample was then centrifuged at top speed for 10 minutes and the flow through collected. The flow through was treated with equal parts phenol and chloroform, centrifuged for 3 minutes at top speed and the top layer was collected. DNA was then ethanol precipitated as previously indicated, and resuspended in sterile dd$H_2O$.

### 2.1.4 DNA sequencing

DNA sequencing was performed by automated DNA sequencing at the Plant Biotechnology Institute, Saskatoon, SK. Sequencing primers utilized included the BC304 primer for the pGAD424 vector, BC293 for pGBT9, pGEX-5' for the pGEX plasmids and the T7 forward promoter primer for pET30a. All sequencing primers were forward primers and were supplied by the Plant Biotechnology Institute.

## 2.2 Recombinant Protein Expression and Purification

### 2.2.1 Bacterial culture and storage

The *E. coli* strain DH10B (Gibco BRL, Grand Island, NY USA) were used for bacterial transformations and plasmid isolation, and BL21 (DE3) and BL21 (DE3)-RIL (Stratagene, #200131 and #230345, respectively) were utilized for protein overexpression of the Rad5 and Rev1 fragments. Unless otherwise noted, bacteria were grown at 37 °C in LB. LB agar plates were prepared by resuspending LB agar powder (L1500) in dd$H_2O$, autoclaving, and alliquotting approximately 25 mL each into Petri dishes. Plasmid selection was maintained by addition of either Ampicillin (Amp) or Kanamycin (Kan) up to a final concentration of 50 mg/mL. Transformed bacterial cells were prepared for long term storage by incubating overnight at 37 °C in 900 μL LB with the appropriate selective drug. Once grown up, 100 μL of dimethyl sulfoxide (DMSO, EMD Chemicals, MX 1485-6) was added, and cells were placed at -70 °C until needed.

### 2.2.2 Preparation of competent cells

Competent cells were prepared as outlined in the Bio-Rad *E. coli* Pulser manual. Bacterial cells were grown to an $OD_{600\ nm}$ of 0.6 in 1 L of LB media. Cells were pelleted at 3500 rpm, and then resuspended in 10% sterile, cold glycerol. Centrifugation was repeated 4x, reducing the volume for resuspension each time, to a final volume of 4 mL. 25 μL aliquots of cells were divided into 1.5 mL Eppendorf tubes and placed at -70 °C for long term storage.

### 2.2.3 Bacterial transformation by electroporation

Prior to electroporation, bacterial competent cells were thawed on ice, and 1-2 μL (no more than 10% of the volume of cells) of DNA sample was added. The mixture was transferred to a GenePulser Cuvette (Bio-Rad, #165-2089) and allowed to chill on ice for approximately 45 seconds before being loaded into a Bio-Rad *E. coli* Pulser and electroporated with an electrical pulse of 1.8 V. Cells were recovered from the cuvette with 280 μL super optimal broth with

catabolite repression (SOC) (SOC broth, American Biorganics, Inc., Niagra Falls N.Y., Cat. No. A19-8445) (5 g yeast extract, 0.585 g NaCl, 0.9523 g $MgCl_2$, 1.204 g $MgSO_4$, 0.1864 g KCl and 3.603 g of glucose per liter of broth). Cells were placed at 37 °C and allowed to recover for 45 minutes. Following recovery, 100 μL of cell suspension was spread on LB plates containing drug appropriate to the desired plasmid selection and incubated overnight for approximately 16 hours at 37 °C until individual colonies were detectable.

### 2.2.4 Recombinant protein overexpression

#### 2.2.4.1 Plasmid construction for recombinant protein overexpression

The pGEX-Rad5-NT164 construct was constructed by isolation of the Rad5-NT164 encoding sequence from pGAD-Rad5-NT164 utilizing the BamHI and SalI restriction sites at the 5' and 3' ends, respectively. The fragment was cut out from pGAD424 and inserted into pGEX6p-3 with these restriction sites. The constructed plasmid was confirmed by restriction digest by *Bam*HI and *Sal*I and agarose gel electrophoresis. Plasmid DNA was then transformed into *E. coli* BL21 (DE3) cells and selected for via LB + Amp plates. The pET-Rev1-CT150 and pGEX-Rev1-CT150 constructs were created similarly to pGEX-Rad5-NT164. The region encoding Rev1-CT150 was transferred from pGAD-Rev1-CT150 to pGEX6p-3 and pET30a utilizing the *Bam*HI and *Eco*RI restriction sites, and confirmed by the same method as above. Each plasmid was transformed into BL21 (DE3) and BL21 (DE3)-RIL cells and plated on LB + Can or LB + Amp as appropriate.

#### 2.2.4.2 Small scale recombinant protein overexpression

For small scale protein overexpression a 10 mL LB + Amp liquid culture was inoculated from a single colony and incubated overnight. In the morning the cells were subcultured 1:50

into 50 mL fresh LB with drug selection, which was grown up to an optical density ($OD_{600nm}$) of 0.6 – 0.8. Cells were then induced with 0.5 – 1.0 mM UltraPure™ Isopropylthio-b-D-galactoside (IPTG) (Invitrogen, Cat. No. 15529-019) for 4 hours, or 0.1 mM IPTG overnight at either 37°C or room temperature (as indicated in Chapter Three). Induced cells were collected by centrifugation and resuspended in 2 mL phosphate buffered saline (PBS) to which 50 μL of lysozyme (10 mg/mL) was added. Cells were allowed to lyse for 5 minutes on ice, then centrifuged for 10 minutes at 13,200 rpm and the supernatant collected. Samples were collected prior to IPTG induction (whole cell uninduced), following lysis (whole cell induced), and from the supernatant (soluble fraction) and pellet (insoluble fraction) following the final centrifugation for analysis by SDS-PAGE.

#### 2.2.4.3 Large scale recombinant protein overexpression and purification

Large scale protein overexpression was only performed for the GST-Rad-NT164 fragment expressed from pGEX-Rad5-NT164. A single colony was used to inoculate a 10 mL overnight culture as above. The 10 mL overnight culture was inoculated into 300 mL fresh LB + Amp and grown up for approximately 4 hours. The 300 mL culture was then inoculated into 2 L of fresh LB + Amp and allowed to grow to an $OD_{600}$ of 0.6 - 0.8. Cells were harvested at 8,000rpm in an Avanti Beckman JA10.5 rotor for 5 minutes and resuspended in 200 mL chilled PBS. Cells were lysed utilizing a cell disruptor and the soluble fraction (supernatant) was collected by centrifugation at 16,000 rpm in an Avanti Beckman JA17 rotor for 30 minutes. Soluble extract was first passed through glass wool then loaded on a glutathione sepharose (glutathione sepharose 4B, GE Healthcare, Cat. No. 17-0756-01) column with a volume of approximately 5 mL. The column was then washed with approximately 5x volume of PBS, and GST-Rad5-NT164 was then eluted from the column with reduced glutathione elution buffer (10

mM L-Glutathione, Sigma, G4251). The sample was concentrated with an Amicon® Ultra-15 Centrifugal Filter Device (Millipore, Cat. No. UFC901024) then dialyzed into cleavage buffer (50 mM Tris, 100 mM NaCl, 1 mM EDTA, pH 8.0). Protein concentration was determined by a BCA™ Protein Assay kit (Amersham Pharmacia Biotech, Inc., 27-0843-01) and the protein was cleaved with 1 μL PreScission Protease (supplied by Dr. Stan Moore) per 100 μg of protein. Cleaved sample was dialyzed back into PBS and re-run on the glutathione sepharose column, with the initial flow through collected in order to eliminate the cleaved GST. The final protein sample was concentrated as above, and subjected to SDS-PAGE analysis to determine the success of purification.

### 2.2.5 Protein analysis

#### 2.2.5.1 SDS-PAGE

Proteins were visualized by sodium dodecyl sulfate polyacrylamide gel electrophoresis (SDS-PAGE) as described in Maniatas *et al*. (Maniatas et al., 1989) in the Mini-Protean 3 gel apparatus. Gels with a 12% resolving layer (Per gel to be made: 2 mL of 30% acrylamide:bis-acrylamide (Sigma, #A-6050), 1.3 mL 1.5 M Tris, pH 8.8 (Tris Amino ultra pure, Angus Buffers and Biochemicals, Niagra, N.Y., Cat. No. 15-40500), 50 μL of 10 % ammonium persulfate (APS) (Sigma, A9164), 50 μL SDS and 4 μL of N,N,N',N'-tetramethylethylenediamine (TEMED) (Sigma, T9281) in a total volume of 5 mL), a 5% stacking layer (330 μL 30% acrylamide:bis-acrylamide, 250 μL 1.5 M Tris, pH 6.8, 20 μL of 10% APS, 20 μL of 10% SDS and 4 μL of TEMED in a final volume of 2 mL) and a thickness of 1 mm were utilized for analysis of the GST-Rad5-NT164 and GST-Rev1-CT150 fusion proteins (expressed from pGEX6p vectors), and a 15% resolving layer (2.5 mL 30% acrylamide:bis-acrylamide, 1.3 mL

1.5 M Tris, pH 8.8, 50 µL of 10% APS, 50 µL of 10% SDS and 6 µL of TEMED in a final volume of 5 mL) and 5% stacking layer were utilized for separation of the $His_6$-Rev1-CT150 fragment (expressed from pET30a). Protein samples were diluted 1:1 in Laemmli sample buffer (Bio-Rad, #161-0737), and 20 µL were loaded onto the gels alongside the Precission Plus Protein™ dual colour standard (Bio-Rad, #161-0374). Gels were electrophoresed at 128 V until the protein of interest travelled approximately half way through the gel. Gels were stained with Coomassie Blue (0.025% Coomassie Brilliant Blue R250, 40% methanol and 7% glacial acetic acid) for approximately 30 minutes, and then incubated in destain solution (40% methanol and 10% glacial acetic acid) until individual protein bands became visible.

#### 2.2.5.2 Western blotting analysis

SDS-PAGE gels were soaked in transfer buffer (6.07 g Tris-base, 28.5 g glycine, 150 mg SDS and 150 mL made up to a total volume of 1 L in $ddH_2O$) before proteins were transferred to Polyscreen® polyvinylidene fluoride (PVDF) transfer membrane (Perkin Elmer, Cat. No. NEF1002001PK) via wet transfer. Transfer was performed over 2 hours at 100 V at 4 °C on ice utilizing the Bio-Rad wet transfer system. The transfer buffer and ice was changed half way through the transfer to maintain efficient transfer. The membrane was blocked overnight in 10% skim milk (Carnation instant skim milk powder) in PBS plus 0.05% Tween 20 (PBST) (Tween®20 Polyoxyethylene 20 Sorbitan Monolaurate, EMD Chemicals, #9480), then incubated with primary antibody specific to the tag of the recombinant protein being analyzed at a 1:10,000 dilution for 1 hour (goat α-GST (GE Healthcare, #27-4577-01) or rabbit α-his (Santa Cruz Biotechnology, #SC-803)). Following primary antibody treatment, the membrane was washed for 30 minutes in PBST, changing the PBST every 10 minutes, then incubated with the secondary antibody (bovine α-goat HRP (Santa Cruz Biotechnology, #SC-2350) or goat α-rabbit

HRP (Santa Cruz biotechnology, #SC-2004)) for 1 hour at a 1:10,000 dilution. The membrane was washed for another 30 minutes as above before visualization by Western Lightning Plus-ECL (Perkin and Elmer Life Sciences, NEL #104) on HyBlot CL autoradiograph film (Denville Scientific, Inc., Cat. No. E3018) with appropriate exposure times.

## 2.3 Yeast Genetics

### 2.3.1 Yeast cell culture

Yeast strains requiring selection were cultured in synthetic dextrose (SD) medium (0.67% Bacto-yeast nitrogen base without amino acids, carbohydrate and with ammonium sulphate, (US Biological, C7082704) and 2% glucose dissolved in dd$H_2O$) supplemented with required amino acids for growth (Sherman *et al*., 1983). For SD agar, 2% bacto-agar (Becton, Dickinson and Company, #214010) was included in the mixture and 25 mL portions were aliquoted into Petri dishes. When selection was not required, yeast cells were cultured in rich yeast-extract peptone dextrose (YPD) broth (US Biological, C7062642) containing 1% Bacto-yeast extract, 2% Bacto-peptone and 2% glucose, or on YPD agar plates (US Biological, C9031173). Yeast cells were placed at -70 °C in sterile 15% (v/v) glycerol for long term storage.

### 2.3.2 Yeast strains

The *S. cerevisiae* strains utilized in this study were isogenic derivatives of either the haploid DBY74 strain or, primarily, the HK578 strain. HK578 is derived from the W303 yeast strain corrected for the *RAD5* gene by Dr. J Klein (New York University). DBY747 was supplied to our group by D. Botstein (Stanford University). The strains derivatives included in this study were created through by gene disruption. The yeast strains utilized here are listed in

Table 2.2. Newly created strains were confirmed based on both phenotypic changes and PCR of the genomic DNA.

### 2.3.3 Yeast transformation

Yeast transformations were performed according to a modified lithium acetate method (Ito et al., 1983). 2 mL yeast cultures were incubated overnight at 30 °C in rich YPD broth, and subsequently subcultured into 8 mL of fresh YPD broth (for a total culture volume of 10 mL) in the morning. Cells were subcultured for approximately 4 hours until mid-logarithmic growth was reached. Cells were dispensed in 1.5 mL volumes into Eppendorf tubes for each transformation to be performed. Cells were collected by centrifugation, washed in 400 µL lithium acetate (LiOAc) solution (0.1 M LiOAc, 10 mM Tris-HCl, pH 8.0 and 1 mM EDTA), and then resuspended in 100 µL LiOAc solution. 2 µL of transforming plasmid DNA and 4 µL of carrier DNA (single-stranded salmon sperm DNA, boiled for 5 minutes prior to use to ensure denaturation) were added to the cells, mixed by inversion, and the mixture was left to sit at room temperature. To maintain suspension of the cells in solution during the next step, 280 µL of 50% PEG4000 was added to the tube, mixed by inversion, and then the cells were incubated at 30 °C for 45 minutes. 39 µL of DMSO was added to the tubes following incubation, and the cells were heat shocked for 5 minutes at 42 °C. Transformed cells were harvested by centrifugation, washed in 400 µL sterile dd$H_2O$, and resuspended in 100 µL sterile dd$H_2O$. The entire cell population was plated on appropriate SD minimal media for plasmid selection and incubated for 3 days at 30 °C. Subsequent colonies were re-streaked onto fresh selective plates and further incubated for 2 days at 30 °C.

**Table 2.2 - *S. cerevisiae* strains used in this study.**

| Strain | Genotype | Source |
|---|---|---|
| PJ69-4a | *MATa trp1-901 leu2-3,112 ura3-52 his3-200 gal4Δ gal80Δ Met2::GAL7-lacZ LYS2::GAL1-HIS3 GAL2-ADE2* | P. James |
| HK578-10A | *MATa ade2-1 can1-100 his3-11,15 leu2-3,112 trp1-1 ura3-1* | H. Klein |
| HK578-6B | HK578-10D with *rad5Δ::URA3* | H. Klein |
| WXY2925 | HK578-10D with *rad5Δ::URA3 rad18Δ::TRP1* | Lab stock |
| WXY971 | HK578-10D with *rad18Δ::TRP1* | Lab stock |
| WXY3034 | HK578-10A with *rad5Δ::URA3 srs2Δ::LEU2* | Lab stock |
| WXY1247 | HK578-10A with *srs2Δ::LUE2* | Lab stock |
| WXY3023 | HK578-10A with *pol30-K164R rad5Δ::HIS3* | Lab stock |
| WXY994 | HK578-10A with *pol30-K164R* | Lab stock |
| DBY747 | *MATa his3-Δ1 leu2-3,112 trp1-289 ura3-52* | D. Botstein |
| WXY731 | DBY747 with *rad5Δ::HUH* | Lab stock |
| WXY3032 | DBY747 with *rad5ΔHUH rad18Δ::LEU2* | Lab stock |
| WXY482 | DBY747 with *rad18Δ::LEU2* | Lab stock |
| WXY3031 | DBY747 with *rad5ΔHUH srs2Δ::LEU2* | Lab stock |
| WXY683 | DBY747 with *srs2Δ::LEU2* | Lab stock |
| WXY3033 | DBY747 with *pol30-K164R rad5Δ::HIS3* | Lab stock |
| WXY2384 | DBY747 with *pol30-K164R* | Lab stock |

Plasmids are listed in Table 2.3. Four main vectors were utilized in this study. The yeast two-hybrid plasmids utilized were, pGAD424 (plasmid map available online at http://www.addgene.org/vector-database/2819/) and pGBT9 (plasmid map available at https://www.addgene.org/vector-database/2828/). The pGEX6p-1 and pGEX6p-3 vectors (maps available at https://www.gelifesciences.com/gehcls_images/GELS/Related%20Content/Files/1314774443672/litdoc28919162AC_20110831100927.pdf) and pET30a vector (map at http://www.synthesisgene.com/vector/pET-30a.pdf) were employed for protein overexpression studies in *E. coli*.

**Table 2.3 - Plasmids employed in this study.**

| Plasmid | Source |
|---|---|
| pGAD424 | S. Fields |
| pGAD *RAD5* | Lab stock |
| pGAD *RAD5-HIRAN* | Lab stock |
| pGAD *RAD5-NT164* | Lab stock |
| pGAD *RAD5-87-164* | Lab stock |
| pGAD *RAD5-51-132* | Lab stock |
| pGAD *RAD5-NT60* | Q. Feng |
| pGAD *RAD5-30-60* | Q. Feng |
| pGAD *RAD5-15-45* | Q. Feng |
| pGAD *RAD5-NT30* | Q. Feng |
| pGAD *RAD5-AA* | L. Ball |
| pGAD *RAD5-I916A* | L. Ball |
| pGAD *RAD5-ΔNT60* | X. Xu |
| pGAD *REV1* | Lab stock |
| pGAD *REV1-CT238* | Q. Feng |
| pGAD *REV1-CT150* | Q. Feng |
| pGBT9 | D. Geitz |
| pGBT *RAD5* | Lab stock |
| pGBT *RAD5-ΔSpeI* | L. Ball |
| pGBT *RAD5-ΔBamHI-NruI* | L. Ball |
| pGBT *RAD5-ΔNruI-SalI* | L. Ball |
| pGBT *RAD5-NcoI-NruI* | L. Ball |
| pGBT *RAD5-ΔNruI-SalI* | L. Ball |
| pGBT *RAD5-HIRAN* | Lab stock |
| pGBT *RAD5-NT164* | Lab stock |
| pGBT *RAD5-87-164* | Lab stock |
| pGBT *RAD5-51-132* | Lab stock |
| pGBT *RAD5-NT60* | Q. Feng |
| pGBT *RAD5-30-60* | Q. Feng |
| pGBT *RAD5-15-45* | Q. Feng |
| pGBT *RAD5-NT30* | Q. Feng |
| pGBT *REV1* | Lab stock |
| pGBT *REV1-CT138* | Q. Feng |
| pGBT *REV1-CT150* | Q. Feng |
| pGEX *RAD5-NT164* | Lab stock |
| pET30a *REV1-CT150* | Q. Feng |
| pGEX *REV1-CT150* | Q. Feng |
| *prad5Δ::HIS3* | W. Xiao |
| *prad18Δ::LEU2* | W. Xiao |
| *prad18Δ::TRP1* | W. Xiao |
| *psrs2Δ::LEU2* | F. Fabre |

### 2.3.4 Targeted gene disruption

Yeast strains were created by targeted gene disruption utilizing disruption cassettes transformed into the cells. Disruption cassettes were prepared by restriction digestion of the plasmid DNA as indicated for each disruption cassette. The disruption cassettes utilized in this study are listed in Table 2.3. The *rad5Δ::HIS3* disruption cassette was released by digestion with *EcoRI* and *SalI* prior to yeast transformation. The *rad18Δ::LEU2* disruption cassette was prepared by digesting with *BamHI* and *HpaI* and the *rad18Δ::TRP1* disruption cassette was digested with *EcoRI* and *XbaI*. The *srs2Δ::LEU2* disruption cassette prepared for transformation utilizing *PstI* for the digestion. 2 µL of each disruption cassette was transformed into the yeast cells.

### 2.3.5 Isolation of genomic DNA

Genomic DNA was prepared from a 2 mL overnight culture of the appropriate yeast strain grown in rich or selective media as required. Cells were harvested by centrifugation in a 2 mL screw cap tube and resuspended in 230 µL of yeast DNA extraction solution (components). 100 µL each of phenol and chloroform were added to the resuspended cells, along with approximately 0.3 g of acid washed glass beads. Samples were lysed by vortexing at top speed for 3 minutes. The tubes were subsequently centrifuged at top speed for 6 minutes, and the supernatant was carefully collected, avoiding disturbance of the layer below. In a fresh tube, 5 µL of NaCl and two volumes of cold 95% ethanol were added to the samples, and the mixture was placed at -20 °C for a minimum of 30 minutes. The precipitated sample was centrifuged at top speed for 15 minutes, and the resultant supernatant was poured off and the pellet allowed to dry completely. The dry pellet was resuspended in 200 µL TE (10 mM Tris-HCl and 1 mM

EDTA, pH 8.0) and treated with 5 µL 10 mg/ml RNase A for 10 minutes at 37 °C. The samples were ethanol precipitated with two volumes of cold 95% ethanol and 8 µL NaCl as before. The ethanol precipitated DNA was pelletted and dried as above, and resuspended in 50 µL sterile $ddH_2O$ (Hoffman and Winston, 1987).

### 2.3.6 Analysis of sensitivity to killing by DNA damaging agents

#### 2.3.6.1 Serial dilution plates

The sensitivity of yeast strains to killing by methyl methanesulfonate (MMS) and UV radiation as previously described (Barbour and Xiao, 2006). MMS infused serial dilution plates were prepared fresh the morning of the experiment to prevent degradation of the drug prior to the experiment. A volume of MMS (Sigma-Aldrich, Cat. No. 129925) appropriate to the desired final concentration was added to 80 mL of autoclaved, molten YPD agar cooled to 55 °C and immediately poured into a large Petri dish. Untreated YPD agar plates were poured at the same time as a control condition. UV plates were prepared in the same manner as the control plates, and exposed to UV radiation after cells had been spotted on them. Cell cultures were prepared by first growing up strains overnight at 30 °C in rich media. Cell numbers were adjusted to equivalent levels between each culture based on the $OD_{600}$ reading of each. A series of 4 tenfold dilutions in sterile $ddH_2O$ were prepared from the normalized overnight cultures, and 8 µL of the undiluted cells and each dilution were spotted across a serial dilution plate for each MMS concentration and UV dose tested, along with the control plate. UV treatment was performed once the spots on the plates had dried completely. The serial dilution plates were incubated for 2 days at 30 °C, and the UV plates were incubated in the dark to prevent photoreactivation. Plates

were subsequently photographed and analyzed for cell growth of each strain across the DNA damage conditions tested.

#### 2.3.6.2 Gradient plate analysis

The gradient plate assay provides an alternative qualitative measurement of sensitivity to killing by MMS or other DNA damaging chemicals to the serial dilution assay (Barbour and Xiao, 2006). Gradient plates were prepared by pouring two separate layers of YPD agar in a square Petri dish. The first layer was poured and allowed to solidify with the plate tilted up on an angle (Figure 2.1A), and the plate was placed flat (Figure 2.1B) for addition of the second layer (Figure 2.1C). Appropriate amounts of MMS were added to 30 mL of molten, sterile YPD agar cooled to 55 °C and immediately poured as the first layer. Once solidified, the second layer of molten agar without drug was added. The control plate was prepared by simply pouring 60 mL of YPD agar into a square Petri dish. Prior to printing cells on the gradient plates, 400 μL of sterile ddH2O was warmed to 55 °C. 500 μL of molten YPD agar, cooled to and held at 55 °C until needed, was combined with the heated $ddH_2O$ and the mixture was kept at 55 °C until use. In order to print the cultures, 100 μL of cells were combined with the water-agar mixture, mixed briefly by finger vortexing, and immediately poured out across a sterile glass slide. The long edge of a second sterile glass slide was dipped into the cell mixture and used to transfer a narrow line of cells onto each gradient plate (Figure 2.1D) starting with the highest drug concentration and working down to the control plate. The edge of the glass slide was dipped into the cells between printings on each plate. The process was repeated for each strain tested, with the cells not being added to the water-agar mixture until immediately prior to printing on the plate. Plates were incubated at 30 °C for 2 days then photographed and analyzed based on growth across the increasing drug gradient of each plate.

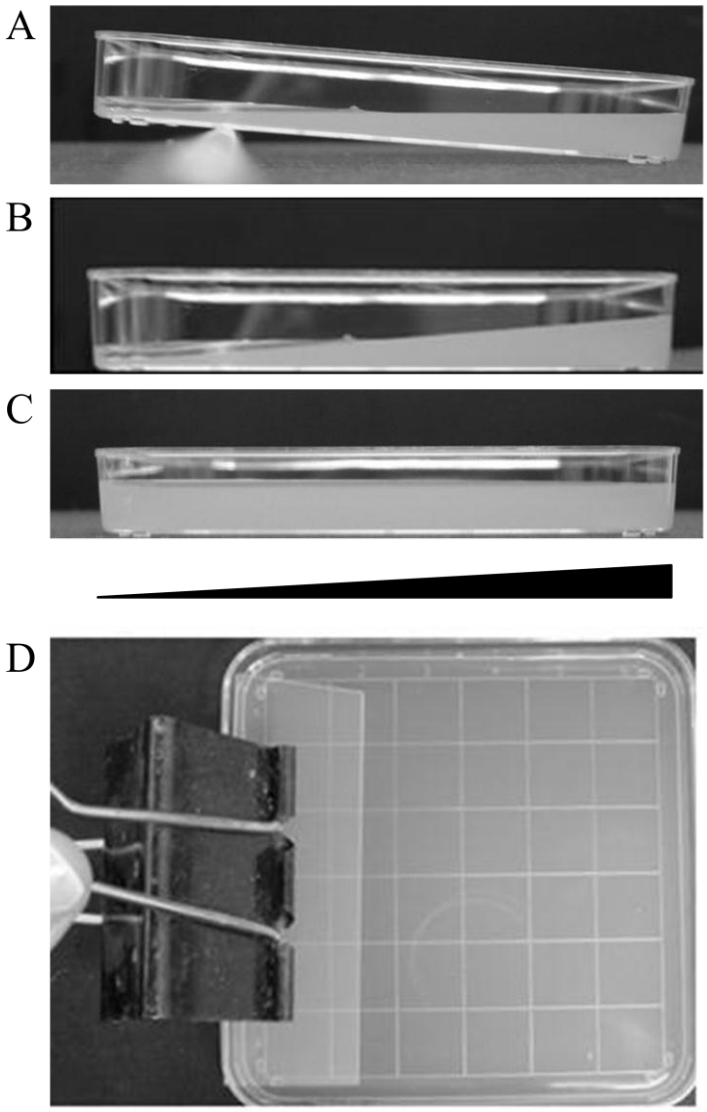


**Figure 2.1 - Construction of gradient plates for qualitative assessment of sensitivity to killing by MMS**. (**A**) The first layer of the gradient plate, consisting of 30 mL of 55 °C molten agar combined with the desired amount of MMS is poured into a square Petri dish tilted up on an angle. Once the first layer has solidified, the dish is placed flat (**B**) and a second layer of molten agar is poured on top of the first, resulting in an even surface (**C**). The triangle below indicates and increasing relative MMS concentration across the plate from left to right. The solidified plate is imprinted with yeast strains in straight lines across the gradient of MMS utilizing the long edge of a sterile microscope slide as shown in (**D**). Plates are incubated for 2 days at 30 °C then analyzed based on growth across the gradient of drug. (Modified from Ball, 2011.)

#### 2.3.6.3 Quantitative liquid killing experiments

For liquid killing experiments, yeast strains were grown overnight in 2 mL of YPD broth at 30 °C. 500 µL of the overnight cultures were inoculated into 5 mL fresh YPD and incubated at 30 °C for 6 hours, until cells reached a density of approximately 2 x $10^7$ cells/mL. 500 µL zero time point samples were taken, and MMS added to the remaining volume of samples to the desired concentration. Samples were centrifuged, washed in 500 mL sterile dd$H_2O$ twice, and 100 µL of each was spread on YPD plates in duplicate. Subsequent samples were taken from the drugged cells at 20, 40 and 60 minute time points, and washed and plated in duplicate as above. Plates were incubated at 30 °C for 3 days, until individual colonies were visible. Colony counts were obtained and averaged between the duplicate plates. The average counts for the drugged samples were scored as percentage of cell survival against the respective untreated, 0 time point strains (Xiao *et al*., 1996). Data is presented as the average of at least 3 independent experiments.

### 2.4 Yeast Two-hybrid (Y2H) Analysis

The Y2H assay was first described by Fields and Song (Fields and Song, 1989), and is performed utilizing the PJ69-4a yeast strain with a combination of $Gal_{AD}$ and $Gal_{BD}$ yeast overexpression vectors (James et al., 1996). The $Gal_{AD}$ and $Gal_{BD}$ plasmids utilized in this study were pGAD424 and pGBT9, respectively. All plasmids utilized in the Y2H assay are listed in Table 2.3. The pGAD-Rad5 plasmid was utilized as the basis for generation of all subsequent Rad5 constructs. All cloning was performed utilizing the *Bam*HI and *Sal*I restriction sites in the multiple cloning sites of both Y2H plasmids. The *RAD5* fragments encoding residues 1-1055, 431-1169, 1-431, 224-431 and 1-223 of the protein were created from pGBT-Rad5 by Dr.

Lindsay Ball in our lab, utilizing unique restriction sites in the gene. Linkers were added where necessary to generate a *Bam*HI restriction site at the 5' ends and a *Sal*I site at the 3' ends of the fragments. The plasmids encoding the Rad5 fragments for residues 1-30, 15-45 and 30-60 were supplied by Qian-qian Feng. All other Rad5 fragments were PCR amplified with the addition of a 5' *Bam*HI restriction site and 3' *Sal*I restriction site in the appropriate oligonucleotides, and cloned into both pGAD424 and pGBT9. The Rev1 fragments utilized in this study were provided by Qian-qian Feng. Appropriate $Gal_{AD}$ and $Gal_{BD}$ plasmids for the interactions assessed were co-transformed into the PJ69-4a yeast strain, and were selected for on SD-Trp-Leu agar, which also serves as the control condition for colony growth in the assay. Plates were incubated for 3 days at 30 °C until individual colonies were visible. Colonies were subsequently re-streaked and incubated for an additional 2 days at 30 °C. Liquid cultures inoculated from the re-streaked colonies were grown to saturation overnight in SD-Trp-Leu media. Cell density as measured at 600 nm was normalized between cultures with additional liquid media to dilute the densest cultures as required. The cultures were spotted on selective agar plates and scored for growth based on the expression of specific Y2H markers. SD-Trp-Leu-His plates (indicated as –His) and SD-Trp-Leu-His + 1 mM or 5 mM 3-aminotriazole (3AT) were utilized to assess activation of the $P_{GAL1}$-*HIS3* reporter gene. 3AT serves as a competitive inhibitor of the product of the *HIS3* gene, and its addition increases the stringency of the selection in media lacking histidine (Serebriiskii *et al*., 2000). SD-Trp-Leu-Ade plates were used to screen for activation of the $P_{GAL1}$-*ADE2* reporter gene. Activation and expression of the reporter genes was scored based on growth or no growth under the respective selective conditions. A minimum of three independently colonies were analyzed for each plasmid combination. Plates were monitored for growth and photographed between 3 and 5 days incubation at 30 °C.

# CHAPTER THREE

## RESULTS

The central goal of this research is to investigate the unknown function(s) of Rad5 within the cell. While Rad5 is clearly involved in error-free DDT, there is significant evidence that it possesses additional functions (Ball, 2011; Gangavarapu et al., 2006; Hoege et al., 2002; Lemontt, 1971; Pages et al., 2008; Unk et al., 2010). A look at the earliest literature regarding Rad5, in addition to the most recent studies, points to an undefined function of the protein within the TLS pathway of DDT in addition to its error-free role (Gangavarapu et al., 2006; Kuang et al., 2013; Lemontt, 1971; Pages et al., 2008). Rad5 physically interacts with numerous components of DDT, including Rad18, PCNA, Ubc13, and interestingly with Rev1 (Carlile et al., 2009; Pages et al., 2008; Ulrich and Jentsch, 2000). Amongst its roles in TLS, Rev1 is thought to function as a scaffolding protein for the other TLS polymerases (Prakash et al., 2005). We suspect this physical interaction holds the key to understanding the unknown functions of Rad5, and likely mediates any TLS activity of the protein. The role of Rad5 in TLS can be better understood by determining the requirements for the interaction with Rev1 and whether its disruption negatively impacts the TLS function of Rad5. With this in mind, our goal was to determine the smallest possible region of Rad5 required to maintain the interaction with Rev1. While the exact role of Rad5 in TLS is not fully understood, the increased sensitivity of *rad5Δ* to killing by DNA damaging agents compared to other mutants in error-free DDT can also be explained if Rad5 acts in a cellular process outside of DDT altogether. In order to verify the placement of *RAD5* solely within the pathways of DDT, we examined the genetic relationship between *rad5Δ* and other genes required for DDT.

## 3.1 Identification of a Putative Rev1 Binding Domain of Rad5 by Yeast Two-Hybrid Analysis

In order to better understand the physical interaction between Rad5 and Rev1 we set out to determine a putative Rev1 binding domain within the Rad5 protein. The yeast two-hybrid (Y2H) assay provides a relatively simple genetic system for screening of protein-protein interactions *in vivo* (Fields and Song, 1989). The system relies on separation of the DNA binding domain ($Gal_{BD}$) and activation domain ($Gal_{AD}$) of a transcriptional activator, which are incorporated into yeast overexpression vectors. The genes encoding the proteins of which the physical interaction is of interest can be cloned into these two vectors, resulting in one protein being fused to the binding domain of the transcriptional activator, and the other fused to activation domain. Should the proteins of interest interact, the activation domain is brought into close proximity to the promoter of a reporter gene, activating transcription and thus expression of the reporter gene. This study utilized reporter genes required for the biosynthesis of both histidine ($P_{GAL1}$-*HIS3*) and adenine ($P_{GAL1}$-*ADE2*) allowing potential interactions to be screened for based on growth in the absence of those nutrients.

Initial Rad5 truncations were created utilizing unique restriction sites within the coding region, and were expressed as $Gal_{BD}$ fusions (constructed by Dr. Lindsay Ball), while full length Rev1 was expressed as a fusion with the activation domain ($Gal_{AD}$). Five truncations of *RAD5* were generated via this method, encoding residues 1-1055, 431-1169, 1-431, 224-431 and 1-223 of the protein (Figure 3.1). Of these truncations, all fragments containing the amino-terminal region of Rad5 (Rad5-1-1005, Rad5-1-431 and Rad5-1-223) demonstrated a positive interaction with *S. cerevisiae* Rev1 based on growth (Figure 3.2).

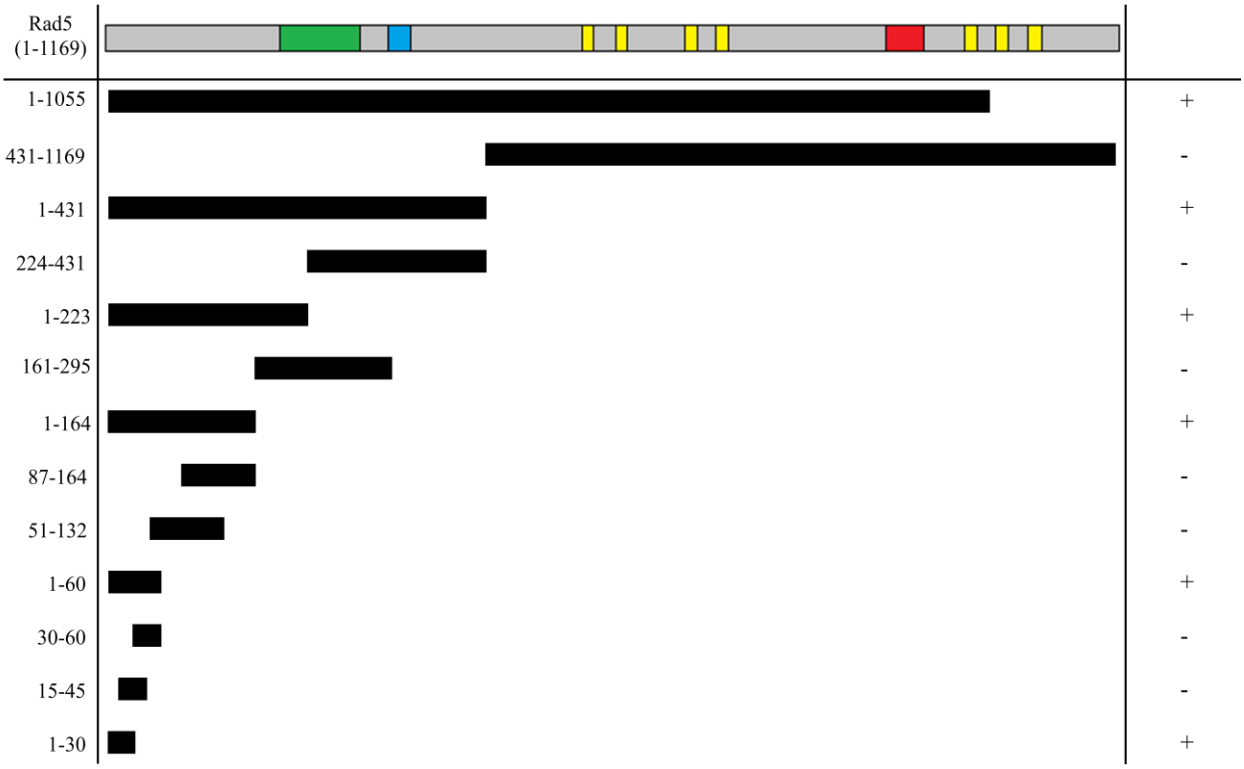


**Figure 3.1 - Rad5 truncations employed for the yeast two-hybrid assays**. The coloured bar indicates the full length Rad5 protein and the relative positions of the domains contained within it. Green indicates the HIRAN domain, blue the leucine heptad repeat, the seven conserved domains marking a SWI2/SNF2 ATPase are depicted in yellow, and the RING finger is represented in red. The relative positions of the various Rad5 truncations utilized for the Y2H experiments in this study are indicated by the black bars, and the numbers indicate the amino acid positions of the constructs. Y2H results are indicated to the right as a + for growth, indicating a protein-protein interaction, and a – for no growth.

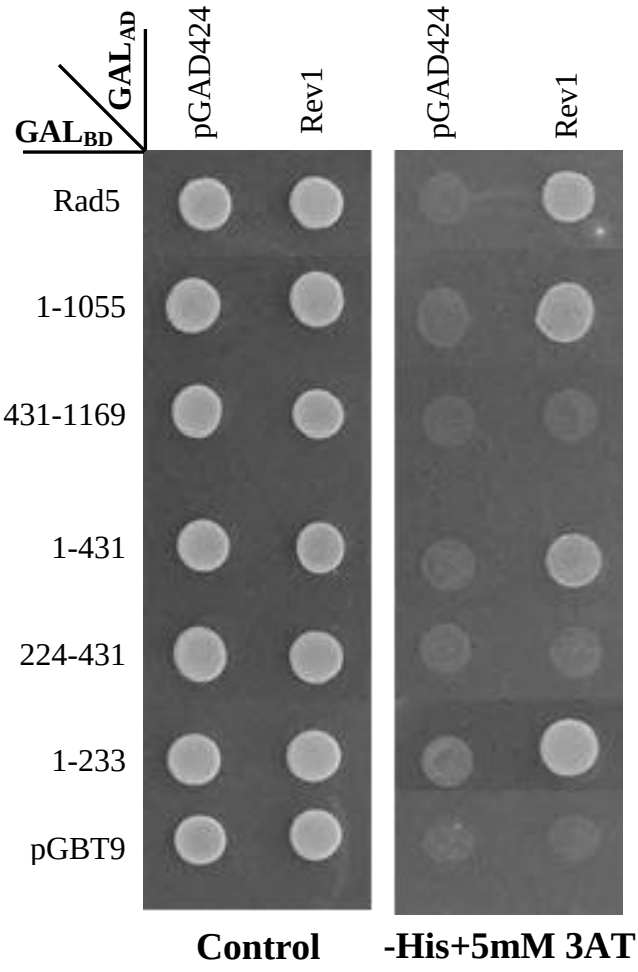


**Figure 3.2 - Identification of an N-terminal Rev1 interacting domain in Rad5 by the yeast two-hybrid assay**. Y2H analysis indicates a positive interaction between the N-terminal containing truncations of Rad5 and Rev1 as indicated by growth on selective media. The yeast strain PJ69-4a was co-transformed with plasmids containing $Gal_{AD}$ and $Gal_{BD}$ fusions, and the various combinations indicated were spotted on control plates selective for maintenance of the plasmids (SD-Trp-Leu) and media selective for a physical interaction (SD-Trp-Leu-His+5mM 3AT). Plates were incubated at 30 °C for 4 days then photographed and scored for growth. A minimum of three independent transformants for each plasmid combination were tested. The numbers indicate the residues of the Rad5 protein being assessed for the interaction with Rev1, with 1 being the N-terminus of the protein.

The HIRAN domain of Rad5 is located around residues 171- 286 (Iyer et al., 2006). The smallest fragment of Rad5 that was positive for an interaction with Rev1 (amino acids 1-223) contains approximately half of the HIRAN domain (Figure 3.1). The HIRAN domain was identified based solely on sequence conservation in the N-terminal regions of several SWI2/SNF2 ATPases and no functions of Rad5 have yet been associated with it (Iyer et al., 2006; Unk et al., 2010). Based on the inclusion of this domain in the Rev1 interacting region of Rad5 identified at this point, two more truncations of *RAD5* were created by PCR amplification to examine whether the HIRAN domain alone was sufficient to interact with Rev1. A fragment encoding residues 161-295 of Rad5 was generated, containing the HIRAN domain and small flanking regions on either side in hopes of allowing proper folding of the domain. A second fragment encoding the N-terminal 164 amino acids was created to account for the region of Rad5 N-terminal to the HIRAN domain indicated as 1-164 (Figure 3.1). These fragments were cloned as both binding domain fusions and activating domain fusions, and were co-transformed with the plasmids overexpressing the appropriate Rev1 fusions for the assay. The results of the Rad5 $Gal_{AD}$ fusions are shown here (Figure 3.3). The Rad5 truncation consisting of the N-terminal 164 residues was positive for growth when co-expressed with Rev1, while the HIRAN domain was negative, indicating that the HIRAN domain is unlikely to be involved in the protein-protein interaction between Rad5 and Rev1. The region of Rad5 N-terminal to the HIRAN domain has no other known activities associated with it (Unk et al., 2010), and a simple BLAST search of the region (http://blast.ncbi.nlm.nih.gov/) indicates that the amino acid sequence is not very well conserved in general.

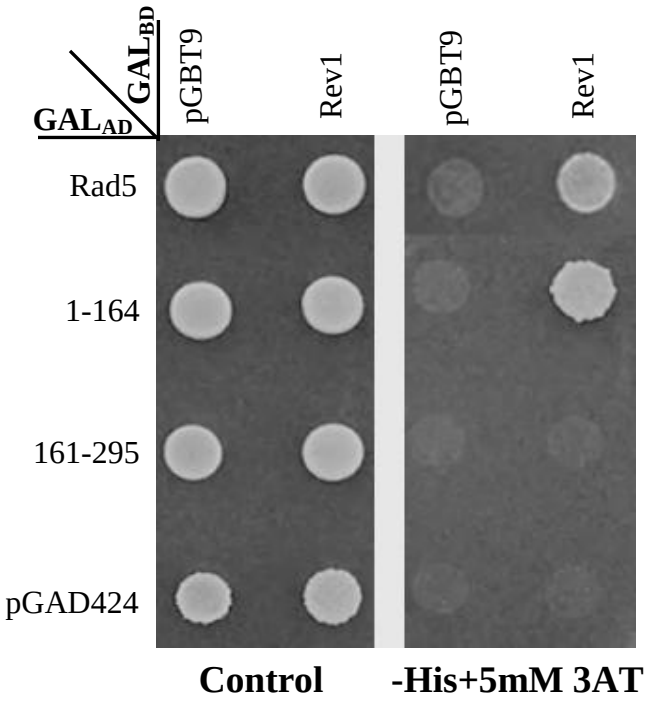


**Figure 3.3 – Yeast two-hybrid analysis of the role of the HIRAN domain in the interaction between Rad5 and Rev1**. The previous assay indicated that the N-terminal 233 amino acids of Rad5 were sufficient to maintain the protein-protein interaction with Rev1. This truncation contained approximately half of the HIRAN domain, and new constructs were designed expressing only the HIRAN domain (indicated as 161-295), and the N-terminal region of the protein up to that point (indicated as 1-164). The numbers refer to the amino acid numbers starting from the N-terminus of Rad5. The Rad5 fragments were assessed as both $Gal_{AD}$ and $Gal_{BD}$ fusions co-transformed with the appropriate *REV1* plasmids, and results were consistent in both experiments. The $Gal_{AD}$ results are shown here as representative of the data. Transformants were plated on selective media as indicated, and photographed following incubation at 30 °C for 4 days. A minimum of three independent colonies from each transformation was assessed.

The N-terminal truncation of Rad5 was further separated into 3 overlapping fragments roughly equal in size by PCR amplification. All fragments were assessed as both binding domain fusions and activating domain fusions for an interaction with the appropriate Rev1 constructs. Y2H analysis of these fragments further narrowed down the putative region required for the physical interaction of Rev1 to the N-terminal 60 residues of Rad5. Figure 3.4 shows the results with the Rad5 constructs in the $Gal_{AD}$ orientation with growth indicating the interaction. The results were identical when the Rad5 constructs were expressed as $Gal_{BD}$ fusions, with the strain transformed with the N-terminal 60 amino acid fragment and Rev1 exhibiting growth on minimal media (data not shown). The N-terminal 60 amino acids were further split into another 3 overlapping fragments (indicated by their amino acid positions as 1-30, 15-45 and 30-60), and analysis revealed that the N-terminal 30 residues were sufficient to maintain the protein interaction of Rad5 with Rev1 as indicated by this genetic assay (Figure 3.5). The results of this sequential determination of a putative Rev1 binding domain in Rad5 are summarized in Figure 3.1.

During the course of these experiments, another group identified a putative Rad5 binding domain within Rev1, also by the Y2H assay (courtesy of Qian-qian Feng). Y2H plasmids expressing the Rev1 C-terminus were contributed to us to determine whether they retained the interaction with the N-terminal truncations of Rad5. The results are depicted in Figure 3.6, and growth on selective media was observed for co-transformants of the Rad5 and Rev1 fragments of interest here, indicative of a physical interaction between the C-terminus of Rev1 and the N-terminus of Rad5.

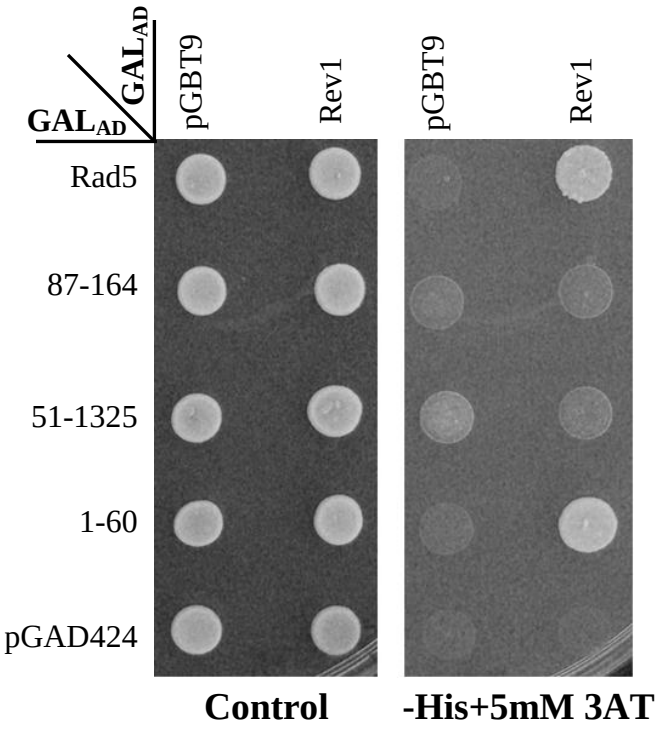


**Figure 3.4 – Yeast two-hybrid analysis of the N-terminal 164 amino acids of Rad5.** Three overlapping fragments were designed based on the N-terminal 164 amino acid fragment of Rad5 that demonstrated a positive Y2H result for an interaction with Rev1. The residues encoded by the three subsequent truncations of *RAD5* are indicated by the numbers above. The fragments were co-transformed in both $Gal_{AD}$ and $Gal_{BD}$ orientations with the appropriate Rev1 protein fusions, and the $Gal_{AD}$ orientation is shown here. Cells were spotted on control plates for growth, and selective media to test the interactions. Photographs were taken after 4 days incubation at 30 °C, and a minimum of three independent transformants for each combination were analyzed. Results were consistent in both plasmid orientations.

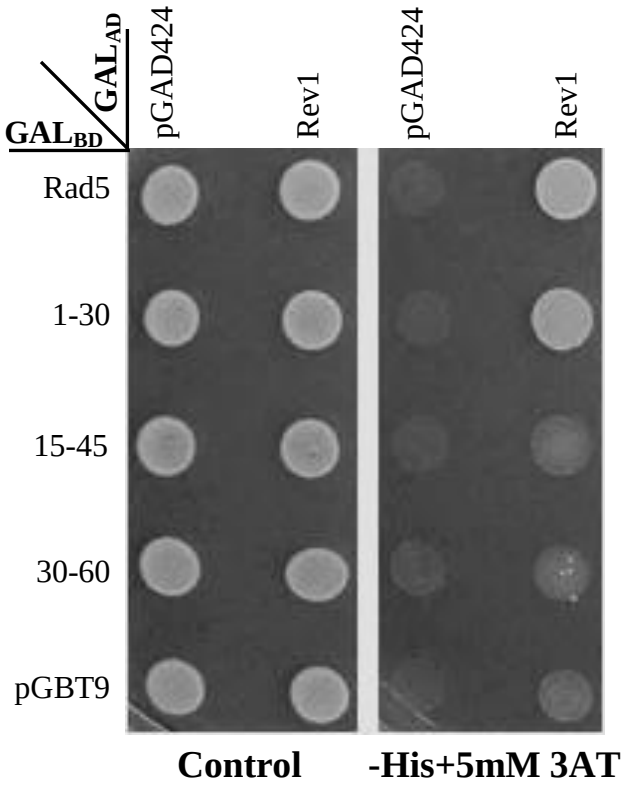


**Figure 3.5 – Analysis of the interaction between the N-terminal 60 residues of Rad5 and Rev1 by the yeast two-hybrid assay.** The region of Rad5 that interacts with Rev1 was narrowed down to the N-terminal 60 amino acids, and further analysis was performed by separating this N-terminal region further into 3 overlapping constructs. The fragments consist of residues 1-30, 15-45 and 30-60 (1 representing the N-terminus) as indicated. The Rad5 fragments were tested as both binding domain and activating domain fusions, co-transformed with the appropriate Rev1 fusions, and results were consistent in both orientations. The Rad5 fragments are shown here in the $Gal_{BD}$ orientation. Cells were incubated on selective media for 4 days at 30 °C then photographed. Growth indicates a positive result, activating expression of the *HIS3* reporter gene.

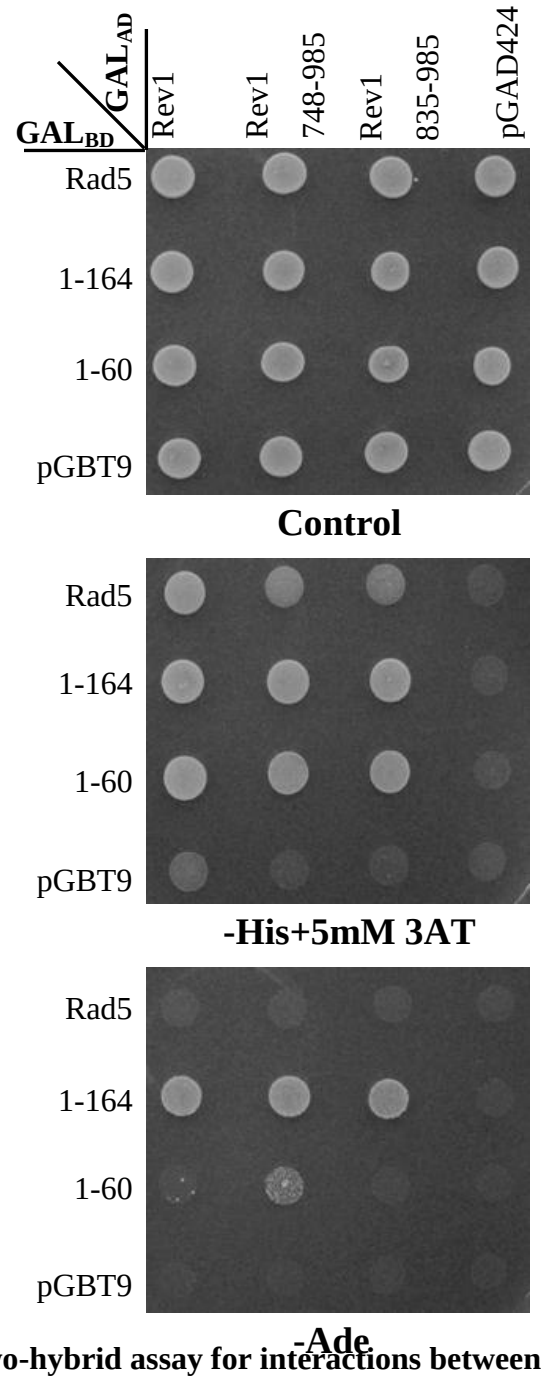


**Figure 3.6 – Yeast two-hybrid assay for interactions between Rad5 and Rev1 truncations.** Rev1 truncations provided by Qian-qian Feng were tested protein-protein for interactions with several of the Rad5 truncations identified to interact with Rev1 in this study by the Y2H assay. Co-transformants in the appropriate combinations were spotted on selective media and incubated for 4 days at 30 °C. Positive results for an interaction were indicated by growth on media lacking adenine or histidine as indicated. Selection on –Ade media is generally considered to have a higher stringency than selection on –His media, even with the addition of 3AT.

### 3.2 Deletion of an N-terminal Region of Rad5

It is interesting that the region identified for an interaction with Rev1 is located directly at the N-terminus of the Rad5 protein. The characterized functions of the protein have all been associated with approximately the C-terminal half of Rad5, and the other "significant" regions in the N-terminal portions prior to this were identified based solely on the sequence and have no verified functional significance (Johnson *et al*., 1992; Iyer *et al*., 2006; Unk *et al*., 2010). With this in mind, it seemed likely that a deletion of the relatively small Rev1 interacting region within Rad5 identified here could abolish this interaction without disrupting the other functions of the protein, such as its ATPase and E3 enzyme activities. A deletion of the N-terminal 60 residues of Rad5 (Rad5-ΔNT60) was constructed via PCR amplification of the gene. A forward primer was designed with homology to the sequences adjacent to the N-terminal 60 residues, and a reverse primer targeted a unique restriction site near the 5' end of the gene. Since the *RAD5* gene is fairly large, amplifying the entire gene would have been challenging. The PCR product was introduced into the full length gene utilizing a restriction site introduced in the forward primer and the unique restriction site targeted by the reverse primer. The N-terminal deletion of Rad5 was constructed by Xin Xu for this study. The construct was assessed for functionality via complementation analysis in comparison to point mutations disrupting the ATPase and E3 activities of the protein (Ball, 2011; Gangavarapu et al., 2006).

Mutations abolishing only the TLS pathway of DDT have little effect on the sensitivity of cells to DNA damaging agents, but drastically reduce levels of induced mutagenesis (Xiao et al., 1999). In contrast, mutations abolishing the error-free pathway of DDT result in a significant sensitivity to DNA damaging agents without disrupting mutagenesis, and in fact result in increased levels of mutagenesis in yeast. A *rad5* null mutation results in an extreme sensitivity

to DNA damaging agents, while point mutations disrupting the ATPase (D681A,E682A; *rad5-D681A,E682A*) and E3 (I916A; *rad5-I916A*) activities of the protein result in a moderate sensitivity similar to other mutations in the error-free pathway of DDT (Gangavarapu et al., 2006). Should the interaction with Rev1 mediate a TLS function of Rad5, a mutation disrupting this interaction would be expected to result in a phenotype similar to a TLS mutation instead of one affecting the error-free branch of DDT.

The pGAD424 yeast expression vector carrying wild type *RAD5*, the N-terminal deletion, and point mutations in the ATPase and RING finger domains were transformed individually into a *rad5* null mutant in an HK578 strain background to assess genetic complementation of the deletion construct in terms of sensitivity to a DNA damaging agent. The complementation assay was assessed qualitatively via the gradient plate assay utilizing MMS as a DNA damaging agent (Figure 3.7). The wild type *RAD5* complemented the null mutant completely, restoring resistance to MMS to the same level as the wild type control, while the point mutations demonstrated the expected moderate sensitivity to the DNA damaging agent. In contrast, the N-terminal deletion construct resulted in a significantly more severe sensitivity than either point mutation. These results indicate that the N-terminal deletion created here likely affects more than just the interaction between Rad5 and Rev1, and is unsuitable for further study into the role of the protein-protein interaction in the function(s) of Rad5.

### 3.3 Expression of the Putative Rev1 Binding Domain of Rad5

While Rad5 and Rev1 are known to physically interact (Pages et al., 2008), the Y2H assay is a genetic method for testing physical interactions, and positive results derived from the

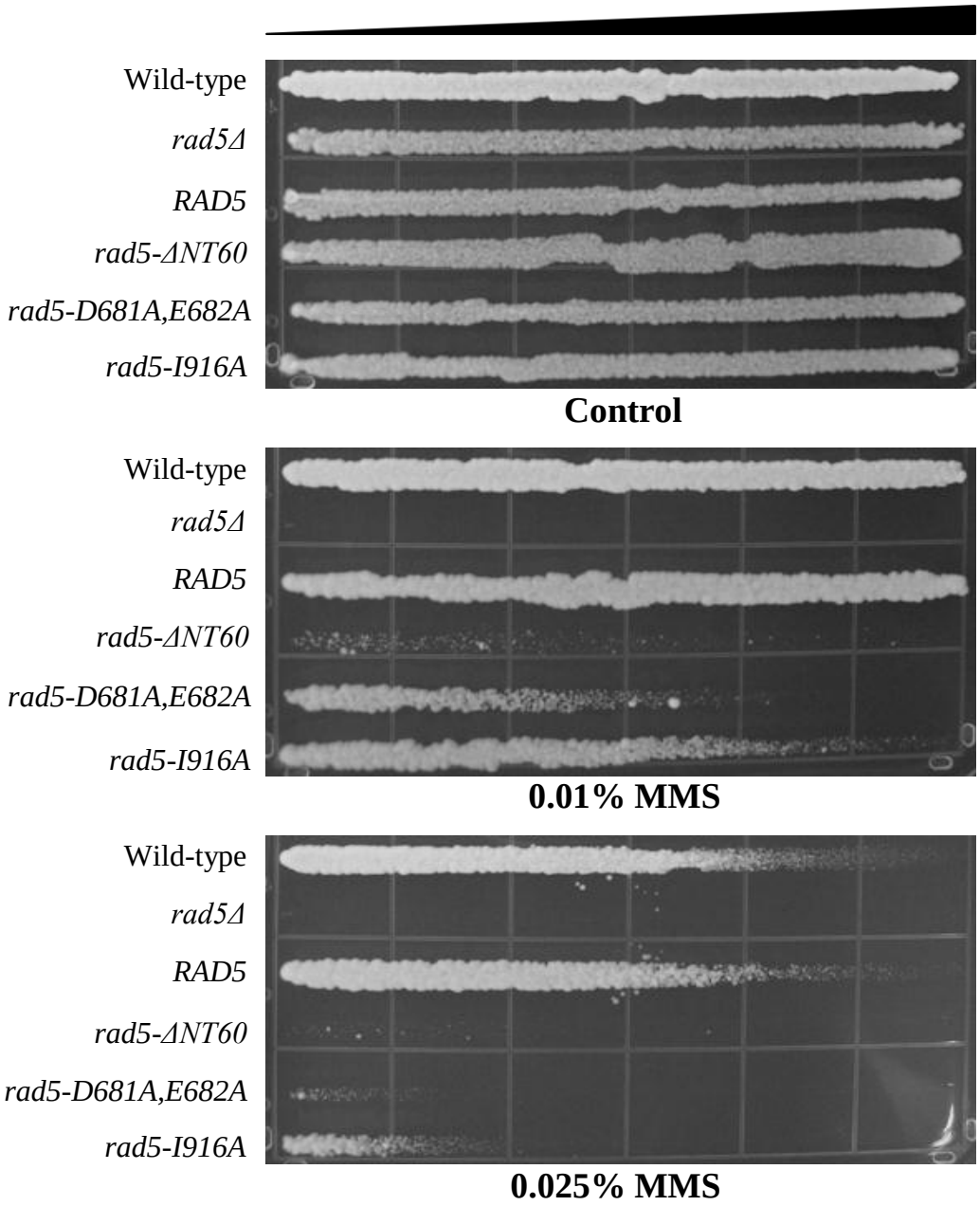


**Figure 3.7 – Complementation analysis of a small N-terminal deletion of *rad5*.** Mutants of the *RAD5* gene were expressed from plasmids in a *rad5Δ* strain isogenic for HK578, and assessed for their ability to rescue the sensitivity to killing by the DNA alkylating agent MMS in a qualitative gradient plate assay. The pGAD424 overexpression vector was utilized to express the mutants in *S. cerevisiae*. Overnight cultures of the transformants were imprinted on YPD alone or YPD with drug. The triangle indicates the increasing gradient of MMS from left to right. Plates were incubated for 2 days at 30 °C and then photographed.

assay are best confirmed utilizing a physical method, such as an *in vitro* pull-down. Subsequently, the protein of interest will need to be overexpressed and purified for physical studies. Purified protein provides an additional opportunity for crystallization and x-ray crystallographic determination the structure of the protein, providing additional detail about the binding region. In order to confirm the Rev1 binding domain of the Rad5 protein the N-terminal 164 amino acid fragment (Rad5-NT164) was selected for expression and purification. This fragment provided a positive result for an interaction with Rev1 across the widest variety of conditions utilized in the Y2H assay (Figure 3.6).

Rad5-NT164 was expressed as a GST tag fusion from the pGEX6p-3 plasmid, and a variety of conditions were tested for optimal overexpression of the recombinant protein as indicated in Table 3.1. Overall, the protein was expressed highly in a soluble form under all induction conditions, and Figure 3.8 is representative of expression levels observed by SDS-PAGE analysis. The identity of the protein was confirmed by Western blot analysis utilizing an α-GST primary antibody (data not shown). Optimal expression levels were obtained with 0.1 mM IPTG treatment overnight at room temperature. With sufficient levels of overexpressed protein, initial purification was attempted for the Rad5 fragment. A purification protocol was planned utilizing affinity chromatography for the GST tag on a column of glutathione sepharose. However, the purification attempted in this study was unsuccessful due to technical issues with the column, and time constraints prevented further troubleshooting and final purification of the protein. The purification of the protein should be relatively simple in the future.

### 3.4 Expression of a Putative Rad5 Binding Domain of Rev1

In order to perform an *in vitro* pull-down to confirm the Rev1 binding domain of Rad5, Rev1 also needs to be expressed. Optimal structural information about the physical binding of Rev1 and Rad5 will be best determined in the future by co-purifying the interacting proteins and crystallizing their bound state. Towards this end a C-terminal fragment of Rev1 that showed evidence of an interaction with Rad5 (Figure 3.6) was selected for protein expression. The Rev1 protein of *S. cerevisiae* is a relatively large protein itself, at 985 amino acids in length, and a truncation of the protein should be easier to manipulate for expression and crystallization. Of the two putative Rad5-interacting fragments, the C-terminal 150 amino acid truncation of Rev1 (Rev1-CT150) was selected for initial expression. This fragment was chosen based on its size similarity to the Rad5 fragment since little difference between the two Rev1 fragments was evident in the Y2H assay (Figure 3.6).

Similarly to the Rad5-NT164 fragment, a variety of expression conditions were assessed as indicated in Table 3.1. Initially Rev1-CT150 was expressed from the pET30a vector with a $His_6$ tag in the BL21 (DE3) *E. coli* cell line. However, expression of the fragment was virtually undetectable in all conditions screened; even via Western blot (data not shown). The fragment was subsequently expressed as a GST-fusion protein from the pGEX6p-3 vector, but expression was still virtually nonexistent. Figure 3.9 demonstrates the typical expression results analyzed by SDS-PAGE. It is clear that this fragment is inappropriate for expression studies, and a different one will need to be selected for further work.

**Table 3.1 - Recombinant protein overexpression conditions.**

| **Rad5-NT164 Overexpression** | | | | | | |
|---|---|---|---|---|---|---|
| Plasmid | *E. coli* Strain | IPTG Concentration (mM) | Induction Time (hours) | Induction Temperature (°C) | Protein Overexpression | Soluble |
| pGEX6p-3 | BL21 (DE3) | 0.5, 0.8, 1.0 | 4 | 37 | + | + |
| pGEX6p-3 | BL21 (DE3) | 0.5, 0.8, 1.0 | 4 | 21 | + | + |
| pGEX6p-3 | BL21 (DE3) | 0.1 | 20 | 21 | ++ | + |

| **Rev1-CT150 Overexpression** | | | | | | |
|---|---|---|---|---|---|---|
| Plasmid | *E. coli* Strain | IPTG Concentration (mM) | Induction Time (hours) | Induction Temperature (°C) | Protein Overexpression | Soluble |
| pET30a | BL21 (DE3) | 0.5, 0.8, 1.0 | 4 | 37 | - | N/A |
| pET30a | BL21 (DE3) | 0.5, 0.8, 1.0 | 4 | 21 | - | N/A |
| pET30a | BL21 (DE3)-RIL | 0.5, 0.8, 1.0 | 4 | 21 | - | N/A |
| pGEX6p-3 | BL21 (DE3)-RIL | 0.5, 0.8, 1.0 | 4 | 21 | +/- | - |
| pGEX6p-3 | BL21 (DE3)-RIL | 0.1 | 20 | 21 | +/- | - |

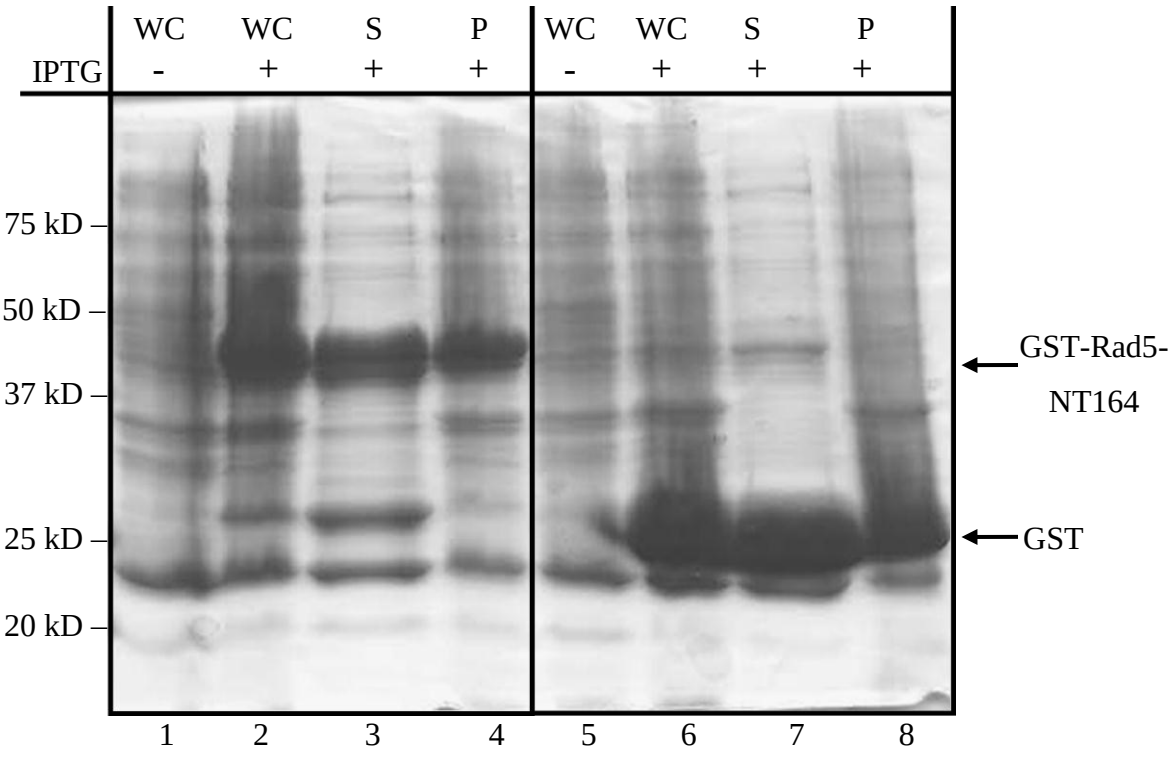


**Figure 3.8 – Expression of the Rad5-NT164 protein fragment.** *E. coli* BL21 cells transformed with pGEX-Rad5-NT164 or the pGEX6p-3 empty vector were subjected to induction with 0.5 mM IPTG for 4 hours at room temperature. Samples taken prior to induction and after induction were run on an SDS-PAGE gel to assess expression levels of GST-Rad5-NT164 compared to the GST tag alone. Bands were visualized following staining by Coomassie Blue. WC indicates a whole cell sample, S refers to the soluble fraction, and P represents the insoluble pellet fraction. IPTG induction is indicated by a +. The expected size of the GST-Rad5-NT164 recombinant protein is 44 kD, and the GST tag alone is 26 kD. Lanes 1 through 4 contain samples from cells transformed with pGEX-Rad5-NT164, and lanes 5 through 8 contain samples from the pGEX6p-3 empty vector transformant. A protein of the expected size for both plasmids is observed in the appropriate lanes.

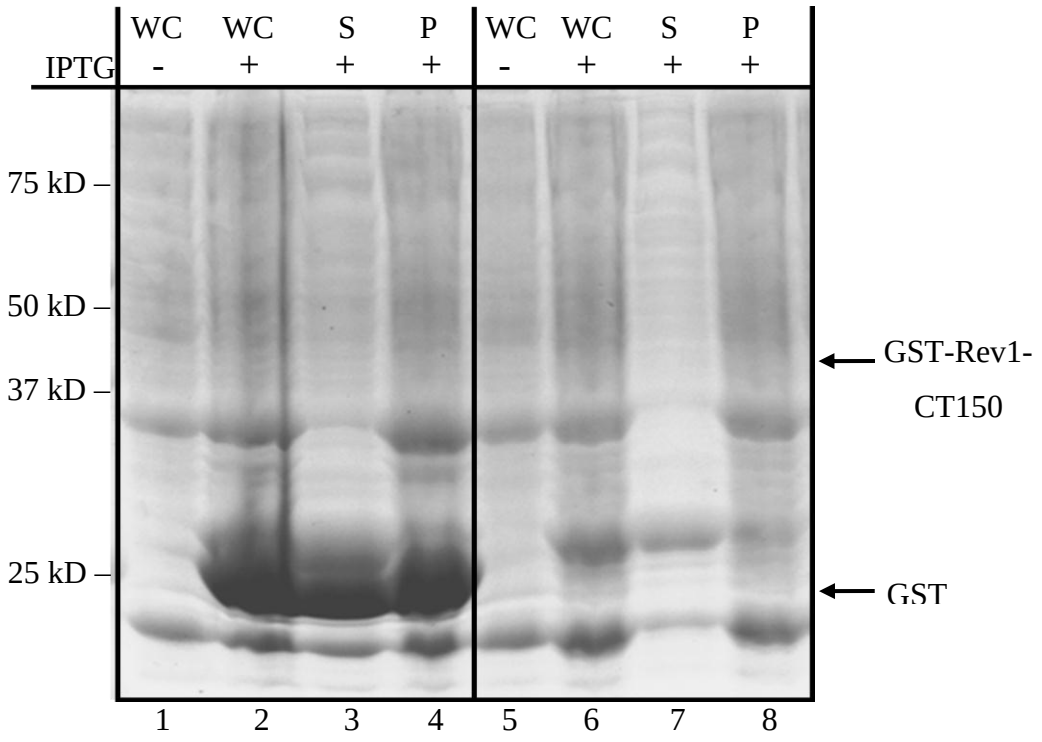


**Figure 3.9 – Expression of the GST-Rev1-CT150 recombinant protein.** *E. coli* BL21 (DE3)-RIL cells were transformed with either pGEX6p-3 (Lanes 1-4) or pGEX-Rev1-CT150 (Lanes 5 and 6). Protein expression was induced by treatment with 0.1 mM IPTG for approximately 20 hours (overnight) at room temperature. Samples were taken prior to induction (indicated by -) and after induction (indicated by +) and run through an SDS-PAGE gels to assess levels of induced protein expression. Bands were visualized by staining with Coomassie Blue. Lanes 1 and 5 contain whole cell (WC) uninduced samples, and lanes 2-4 and 6-7 contain whole cell fractions, soluble fractions (S) and insoluble pellet (P) samples from the induced transformants. Lanes 1-3 show an overexpressed protein approximately the same size as the expected 26 kD GST tag. Lanes 6-7 were expected to contain the GST-Rev1-CT150 recombinant protein (42.5 kD), but no protein expression was observed.

### 3.5 Epistasis Analysis of *rad5* in DDT

While the physical interaction between the Rad5 and Rev1 proteins may shed light on the unidentified function(s) of Rad5 in DDT, it is also possible that the unusual sensitivity of a *rad5* null mutation compared to *mms2Δ* or *ubc13Δ* could be explained by a function for Rad5 outside of DDT altogether. Traditionally, members of the *RAD6* repair group were characterized based on epistasis analysis of the genetic relationships between the components of the pathway (Xiao et al., 1999). An epistatic relationship is observed when the phenotype of a mutation in one gene overrides the phenotype of a mutation in another gene. In other words, the phenotype of the double mutant is identical to the phenotype of one of the single mutants. An epistatic genetic relationship indicates that the two genes are involved in sequential steps of the same biochemical pathway (Friedberg et al., 2006). Alternatively, should the genes mediate steps in different biochemical pathways, mutations in those genes would result in an additive or synergistic phenotype. In terms of DDT, analysis of genetic relationships is determined based on the sensitivity of single and double mutants to killing by DNA damaging agents (Xiao et al., 1999). Null mutations of *rad6* and *rad18* are epistatic to other genes involved in DDT, and as such were placed upstream in the working model for the pathway (Figure 1.2). Combination of mutations in genes in the error-free and TLS branches with each other results in a synergistic phenotype since they mediate separate pathways within DDT, and the sensitivity of the double mutants are similar to the sensitivity of a *rad18* null mutant (Xiao et al., 1999). If Rad5 functions in DDT alone then *rad18Δ* should be epistatic to *rad5Δ* in terms of sensitivity to killing by DNA damaging agents. Should Rad5 play a role outside of DDT, the null mutant would be expected to have an additive sensitivity when combined with *rad18Δ*.

Additionally, activation of DDT requires covalent modification of PCNA at K164 (Hoege et al., 2002). As such, a K164R point mutation prevening the covalent modification of the sliding clamp completely abolishes DDT, and thus demonstrates an epistatic relationship to all genes involved in DDT. *SRS2* also has an interesting relationship to DDT. Normally Srs2 serves to block activation of HR in *S. cerevisiae* at times when HR would be problematic, such as during DNA replication, by preventing the formation of Rad51-ssDNA filaments (Krejci et al., 2003; Veaute et al., 2003). A *srs2* null mutation is epistatic to DDT mutations in a manner dependent on functional HR, suggesting that in the absence of Srs2, HR can be initiated and block activation of DDT (Schiestl et al., 1990). Should Rad5 possess activities only in DDT both *pol30-K164R* and *srs2Δ* should demonstrate an epistatic relationship to *rad5Δ* when assessed for sensitivity to DNA damaging agents.

Epistasis analysis of *rad5Δ* combined with each of *rad18Δ*, *srs2Δ* and *pol30-K164R*, was examined qualitatively utilizing a serial dilution experiment and treatments with both MMS and UV as DNA damaging agents. In this assay strains are spotted in decreasing concentrations across YPD plates, and growth in the presence of a DNA damaging agent is analyzed. The assay was performed with mutants in both an HK578 and DBY747 strain background. Phenotypes were indistinguishable between the two strain backgrounds, and results for the strains isogenic to HK578 are shown in Figure 3.10. According to growth across a range of increasing YPD concentrations and UV doses, *rad5Δ* and *rad18Δ* appeared to have an additive sensitivity since fewer cells of the double mutant strain can grow following DNA damage than either single mutant. Both *srs2Δ* and *pol30-K164R* proved to be epistatic to *rad5Δ* since the respective double mutants exhibit equal growth to the *srs2Δ* and *pol30-K164R* single mutants.

.

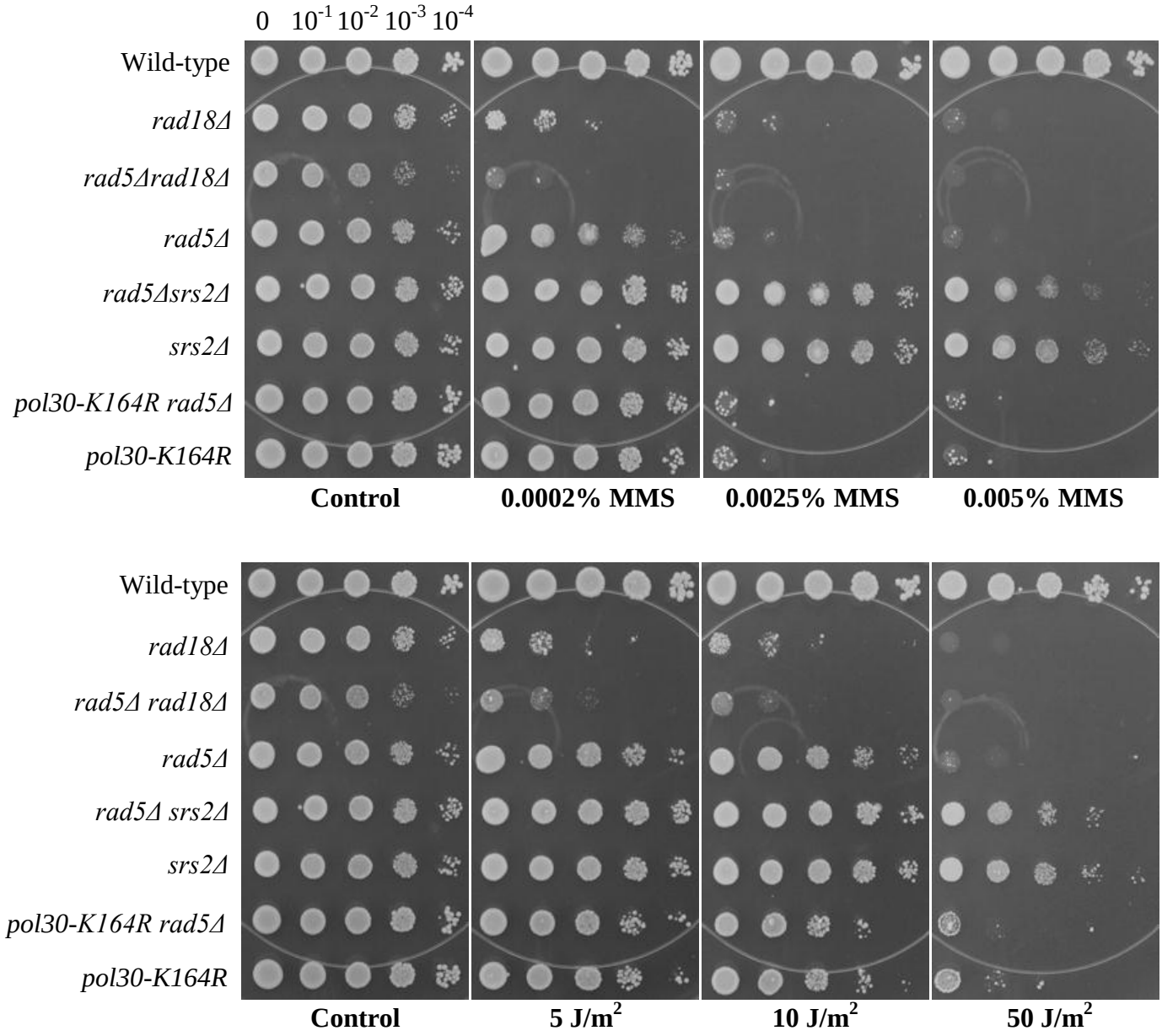


**Figure 3.10 – Genetic interactions with respect to MMS and UV sensitivity between *RAD5* and genes required for activation of DDT in *S. cerevisiae*.** Overnight cultures were spotted on YPD or YPD + various concentrations of MMS and incubated for 2 days at 30 °C. UV treatments were given to spotted plates in the doses indicated, and plates were incubated in the dark to prevent photoreactivation. Photographs were taken following the incubation, and the experiment was repeated independently. All strains were isogenic for the W303 wild-type strain HK578.

The qualitative gradient plate assay was utilized to confirm the genetic interactions between these mutants. Strains isogenic to HK578 were imprinted across YPD plates with increasing gradients of MMS concentrations, and analyzed for growth across the gradient. The genetic relationships were identical to those observed on the serial dilution plates (Figure 3.11). The *rad5Δ rad18Δ* double mutant did not grow as far across the gradient as either single mutant, indicating an additive relationship, while the *rad5Δ srs2* and *pol30-K164R rad5Δ* double mutants grew to an equal distance as the *srs2Δ* and *pol30-K164R* single mutants, respectively. This indicates an epistatic genetic relationship with *SRS2* and *POL30*

Lastly, the genetic interactions of these mutants were determined by a quantitative liquid killing assay, also in MMS. Strains grown in YPD broth were treated with acute doses of MMS appropriate to the expected sensitivities of the mutants. Strains were subsequently plated on YPD plates and survival determined based on the number of viable cells counted as colonies. The *rad5Δ* and *rad18Δ* mutants were confirmed as having an additive relationship based on the increased sensitivity to killing by MMS of the double mutant over the single mutants (Figure 3.12). The *srs2* null mutant rescued the sensitivity of *rad5Δ* to the level of the *srs2Δ* single mutant as observed in the other assays (Figure 3.13), and *rad5Δ* combined with *pol30-K164R* was indistinguishable from either single mutant with respect to killing by MMS (Figure 3.14). This further confirmed that *SRS2* and *POL30* are epistatic to *RAD5*, as would be expected in Rad5 functions solely within DDT. However, since *rad5Δ* and *rad18Δ* mutants consistently exhibited an additive phenotype, it would seem to indicate that Rad5 functions outside of DDT. Taken together, these results were not quite as expected should Rad5 function either outside DDT, or solely within the DDT pathway. These results complicate the current model of DDT, and the implications are discussed in the next chapter.

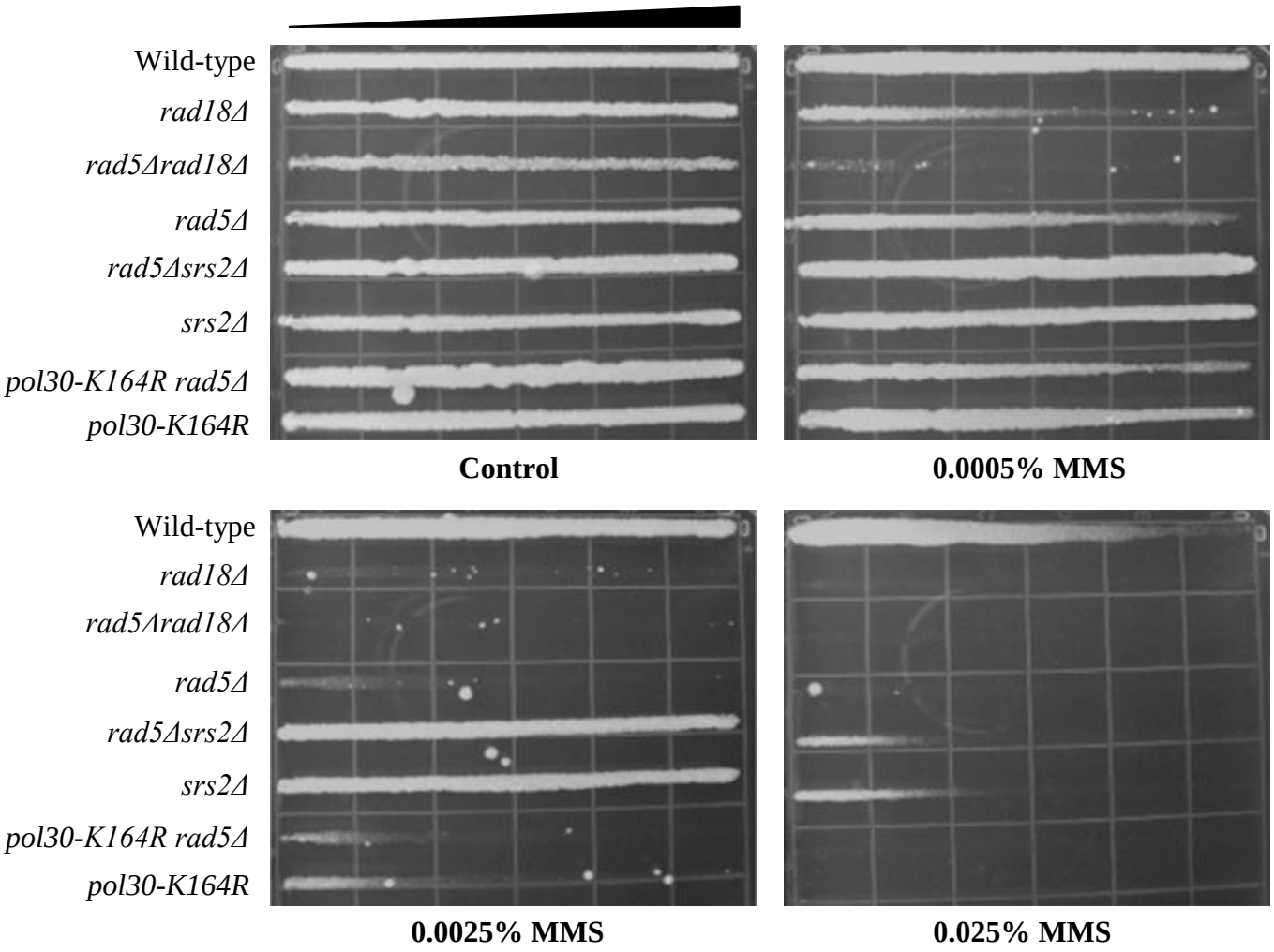


**Figure 3.11 – Genetic interactions between *RAD5* and genes required for activation of DDT in the qualitative gradient plate assay with MMS.** Strains were created in the HK578 background, and were cultured overnight then printed in YPD or YPD + the concentrations of MMS indicated. Strains were imprinted across the gradient increasing from left to right as represented by the triangle. Plates were incubated at 30 °C for 2 days then photographed and analyzed. Two independent replicates of the gradient plate assay were performed.

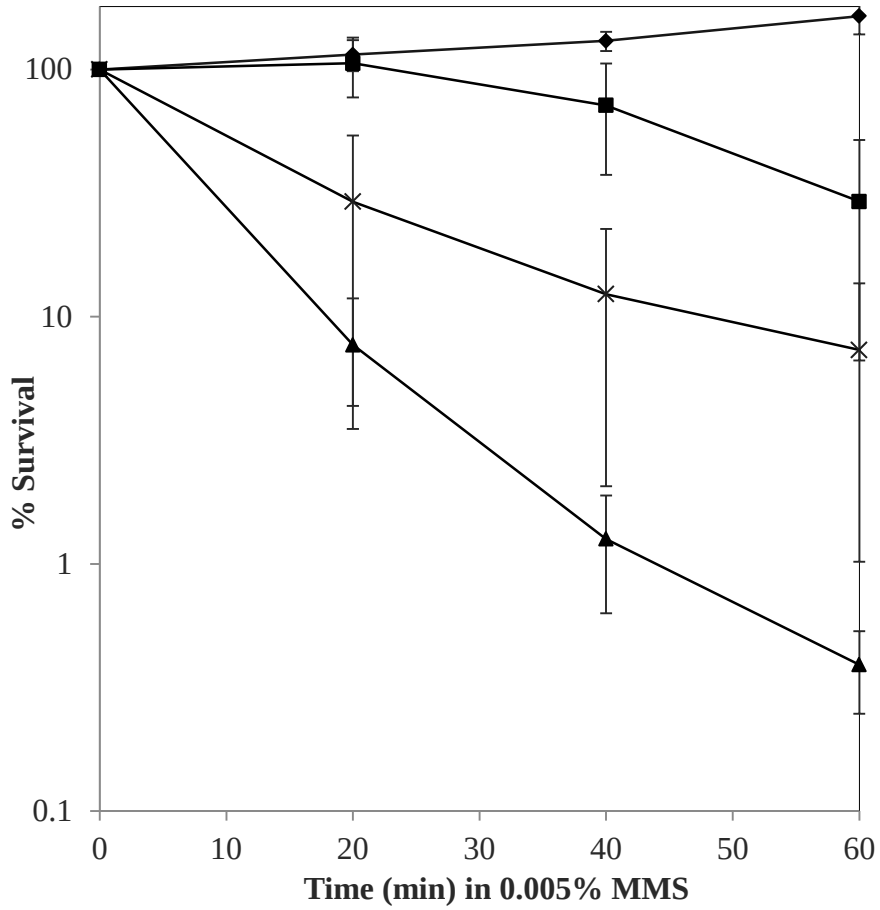


**Figure 3.12 – Epistasis analysis of the sensitivity of a *rad5Δ rad18Δ* to killing by 0.005% MMS in a quantitative liquid killing assay.** The strains were isogenic derivatives of HK578 and are as follows: (◆) HK578-10A (wild-type); (■) *rad5Δ*; (X) *rad18Δ*; (▲) *rad5Δ rad18Δ* . The results are the average of 3 independent experiments. Error bars indicate ±1 standard deviation.

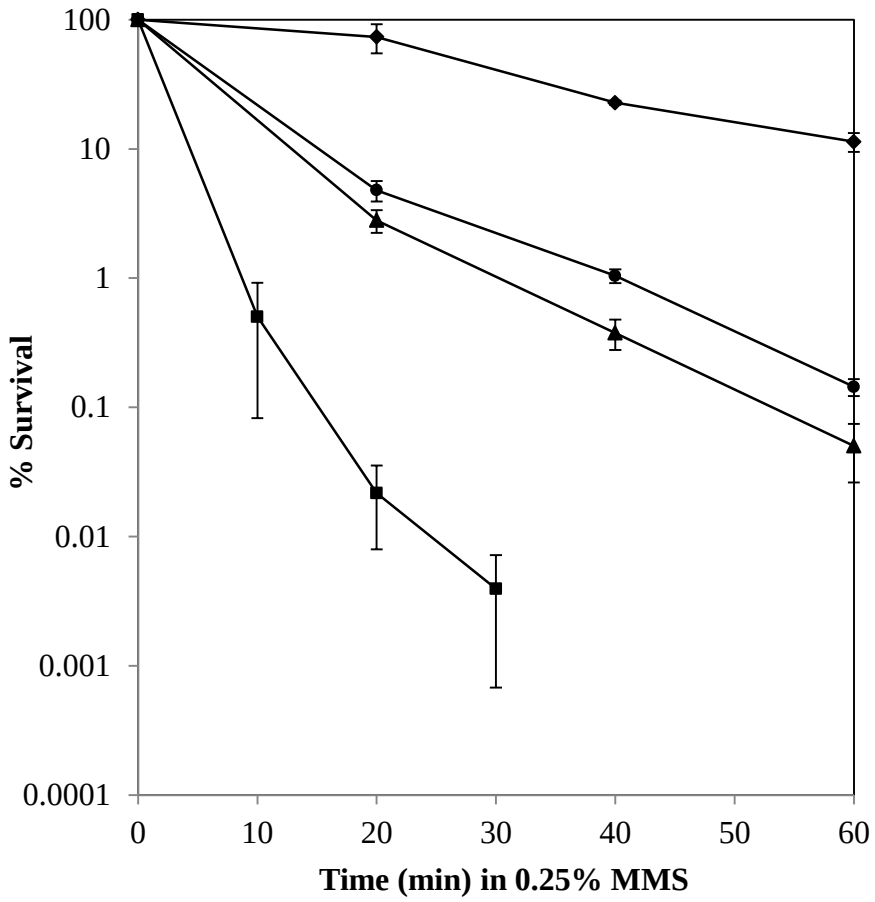


**Figure 3.13 – Liquid killing analysis of the *rad5Δ srs2Δ* mutant treated with the DNA alkylating agent MMS.** All strains utilized were in an HK578 strain background: (◆) HK578-10A (wild-type); (X) *srs2Δ*; (▲) *rad5Δ srs2Δ*; (■) *rad5Δ*. Results were obtained as the average of 3 independent experiments. Error bars indicate ±1 standard deviation.

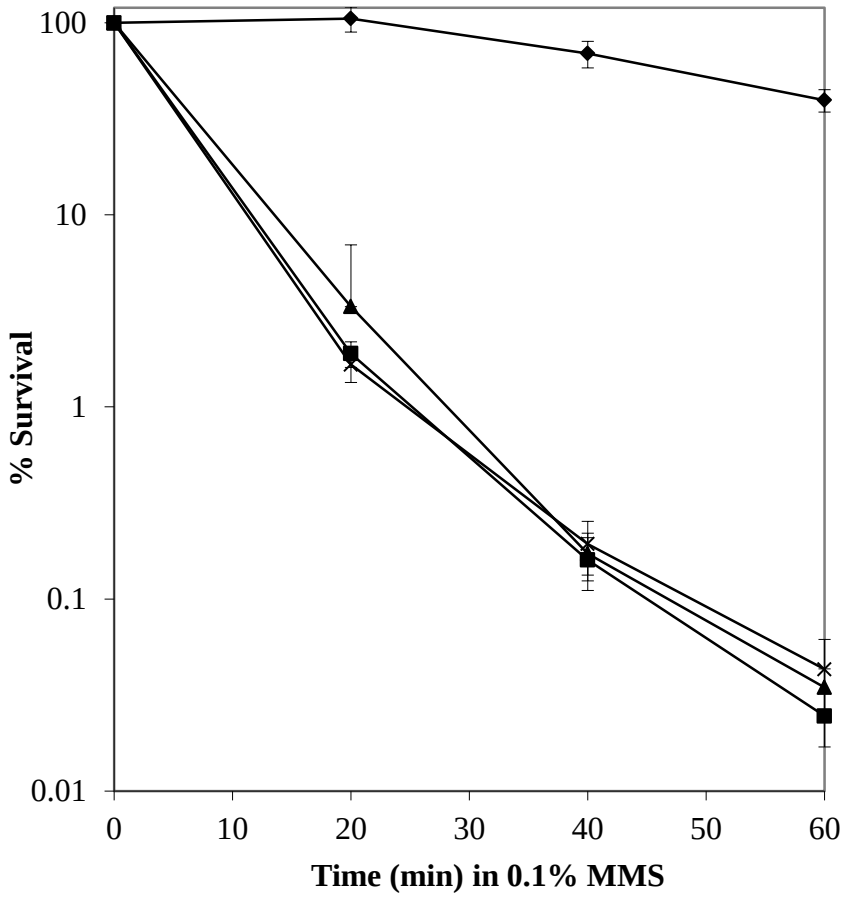


**Figure 3.14 – Quantitative determination of the genetic relationship between *rad5Δ* and *pol30-K164R* with regards to killing by MMS.** The strains tested were derived from an HK578 strain background: (◆) HK578-10A (wild-type); (X) *pol30-K164R*; (▲) *pol30-K164R rad5Δ*; (■) *rad5Δ*. Results were averaged from three independent replicates of the assay. Error bars indicate ±1 standard deviation.

# CHAPTER FOUR

# DISCUSSION

It has become clear that Rad5 must play a role beyond its function as an ATPase and RING finger E3 enzyme in the activation of the error-free mechanism of DDT. The goal of this research was to determine areas in which Rad5 may be acting beyond its already defined roles, based on physical evidence and genetic interactions between *RAD5* and other DDT components.

## 4.1 Definition of a Rev1 Binding Domain within Rad5

While *RAD5* was initially identified as *REV2*, it was later determined that the gene was not actually required for UV mutagenesis (Johnson et al., 1992; Lemontt, 1971). It was thus believed that the initial identification of the gene was a mistake. However, more recent research has made it clear that *RAD5* is indeed required for the promotion of TLS through replication blocking abasic sites in the DNA, as well as (6,4) TT photoproducts, but not for Polη mediated bypass of *cis-sin* TT dimers (Gangavarapu et al., 2006; Pages et al., 2008). It has been theorized that Rad5 may thus be involved in mediating the extension step carried out by Polζ following insertion of a nucleotide opposite the damaged site. Interestingly, a screen for a physical interaction between Rad5 and the TLS enzymes revealed that Rad5 binds only to Rev1, the scaffolding protein of TLS (Pages et al., 2008). Subsequently, it is likely that this physical interaction is critical to the as yet undefined role Rad5 plays in the mechanisms of TLS in *S. cerevisiae*, providing a new approach to determine the uncharacterized function(s) of Rad5.

In this study we confirmed the interaction between Rev1 and Rad5 utilizing the Y2H assay and then proceeded to identify a small region of Rad5 capable of maintaining this interaction located directly at the N-terminus of Rad5. A fragment encoding only the N-terminal

30 residues of the protein was in fact sufficient for an interaction with Rev1 via the Y2H assay. Interestingly, a recent study performed a similar series of experiments also utilizing the Y2H assay, and achieved similar results (Kuang et al., 2013). They determined that deletion of the C-terminal 21 residues of Rev1 was sufficient to disrupt the interaction with Rad5, and loss of the N-terminal 20 residues of Rad5 abolished the interaction with Rev1. In all, they identified a Rad5 interacting domain within Rev1 consisting of residues 351-980, and a Rev1 interacting domain in Rad5 located within residues 21-360. These regions are significantly larger than the domains identified in this study, but the locations are consistent with our results. When examining the results of Kuang and associates (Kuang et al., 2013) in the context of this study of Rad5, it appears that the region of the protein between residues 21-30 contains the key residues for binding to Rev1. Further examination of the role of the interaction on the function of Rad5 in TLS should be directed at this location.

Functional analyses of a Rev1 construct lacking the C-terminal 21 residues indicate that the interaction with Rad5 could be critical to the normal function of Rev1 in TLS bypass of damaged DNA (Kuang et al., 2013). However, the study fails to take into account whether deletion of this C-terminal tail of Rev1 disrupts the activity of the protein via abolishment of the interaction with Rad5, or whether the deletion may have other unforeseen effects on the protein. For instance, it could completely disrupt the structure of the protein or may disrupt other interactions in which Rev1 is involved as a scaffolding protein. The C-terminal region of Rev1 has been associated with both Ub binding and the interaction with the Rev7 subunit of Polζ (Sale et al., 2012). The C-terminal deletion utilized in the study could therefore conceivably abolish the ability of Rev1 to be recruited to stalled replication forks, or disrupt the ability of Rev1 to further assemble the other TLS enzymes for DNA damage bypass.

Similarly we created a deletion construct of Rad5 lacking the N-terminal 60 amino acids in an attempt to determine what role the interaction between Rad5 and Rev1 may play in the TLS function of Rad5. However, a complementation assay in a *rad5Δ* background revealed that loss of the N-terminal 60 amino acids resulted in a greater sensitivity to DNA damage than would be expected if it solely affected TLS within the cell. Rad5 is a multifunctional protein, and this sensitivity to DNA damage could indicate that several of its functions are disrupted. It is possible the N-terminal deletion disrupts the overall folding of the protein, but without any available structures for Rad5 it is difficult to say for certain. Kuang *et al*. (Kuang et al., 2013) did not perform any similar assays to determine the significance of their functional results, and more work is clearly needed to understand the role of the interaction between Rad5 and Rev1 in mediating the mechanisms DDT.

However, the phenotype of the N-terminal deletion of Rad5 may have a different explanation. The association of the C-terminus of Rev1 with protein-protein interactions as part of its role in TLS also has potential implications for an additional role of Rad5 in error-free DDT. Binding of Rad5 to the C-terminus of Rev1 could block binding of Rev1 to PCNA at stalled replication forks, and prevent the assembly of the TLS enzymes for direct bypass of damaged DNA. Simultaneously, Rad5 could recruit Ubc13, and by extension Mms2, for poly-ubiquitination of PCNA and activation of the error-free mechanism of DDT. This would explain the more severe sensitivity of the *rad5* mutant to MMS than would be expected if the mutation only affected the TLS activity of Rad5.

### 4.2 Significance of a Rad5 TLS Activity

The mechanisms employed for DDT are of interest in terms of the development of cancer in humans. While much of the initial research was conducted in yeast, the components of DDT are highly conserved in humans (Ulrich, 2011). DDT can utilize mechanisms which are error-free or are error-prone, and one goal of the research into these mechanisms is to understand how a cell decides between the two pathways. If this decision, and exactly how the branches of DDT are connected, were fully understood it would provide insight into a route through which potential cancer causing mutations may arise in humans. The accepted model of DDT suggests that Rad6 and Rad18 are upstream of the branch between the two branches, and all other components are downstream. However, the model is complicated by the involvement of Rad5 in TLS as well as the error-free mechanism of DNA damage bypass. The function of Rad5 in TLS under specific conditions and the physical interaction with Rev1 imply a level of interconnectedness between the two branches of DDT. Does Rad5 actually act upstream of the branch point between TLS and error-free DDT? The data coming to light would seem to suggest this is possible. Further analysis of how Rad5 connects to TLS will be critical to the goal of understanding how DDT can lead to potentially dangerous mutations, and a better understanding of one mechanism through which cancer may arise in humans.

### 4.3 Expression and Crystallization of the Rev1 Interacting Domain of Rad5

With a relatively small region of Rad5 identified as a potential Rev1 binding domain the next step is to confirm physical binding utilizing another assay such as an *in vitro* pull down. Confirmation of the binding domain will lend to the significance of the Y2H results and future research into the biological function of the physical interaction between Rad5 and Rev1 in the cell. Additionally, since a small N-terminal deletion in the Rad5 protein proved to be unsuitable for functional studies of the role of the interaction, expression and purification of the protein for

further analysis provides an opportunity to further narrow down the key residues in Rad5 for the interaction with Rev1. Both full length Rad5 and Rev1 are large proteins (134 kD and 112 kD, respectively) and no structure has been determined for Rad5, due at least in part to the difficulty of crystallizing such large molecules. Identification of small binding domains provides truncations of the proteins more appropriate for X-ray crystallographic structural studies to determine the residues with which the proteins interact with each other.

A truncation comprised of the N-terminal 164 amino acids of the *S. cerevisiae* Rad5 protein was successfully expressed as GST fusion protein from the pGEX6 vector in *E. coli* BL21 (DE3) cells. The protein was overexpressed under every condition assessed, and in a soluble form, making it ideal as a tool for further study. A GST tag was utilized for ease of future purification and for identification by Western blot for the *in vitro* pull down suggested here. The ease of expression and solubility should also allow sufficient protein to be purified for crystallization. Purification by affinity chromatography for the GST tag should be sufficient for an *in vitro* pull-down assay to confirm the binding of the respective Rad5 and Rev1 interacting domains identified by the Y2H assay. Crystallization, however, requires extremely pure protein and additional purification steps will be required. The pI of the N-terminal 164 amino acids of Rad5 is predicted at 4.42, making the protein an ideal candidate for ion exchange chromatography. Therefore, a purification protocol for crystallization of the Rad5 N-terminal fragment should include initial purification of the recombinant protein by affinity chromatography with the GST tag, followed by cleavage of the tag and further purification of Rad5-NT164 by anion exchange chromatography.

However, even if crystals can be obtained from the purified Rad5 protein fragment, there is no guarantee that they will diffract sufficiently for determination of a protein structure, and

alternative truncations may be required to continue the research. Since the progressively smaller truncations examined in the Y2H assay were all sufficient to maintain an interaction with Rev1, generation of different relevant truncations suitable for crystallization should not be a problem. A BLAST search (http://blast.ncbi.nlm.nih.gov/) with a Rad5 query sequence indicates that a domain boundary appears to exist at around residue 120, since the sequence up to that point shows evidence of some evolutionary conservation. The sequence conservation could imply a region that folds into a specific structure that likely provides the context for the residues involved in the interaction with Rev1. By designing a construct around this region, it will hopefully allow proper folding of the region and thus a relatively immobile structure for crystallization. Alternatively, the HIRAN domain is located from amino acids 171-286, and a Rad5 construct could also be designed based around the C-terminal end of the domain. Again, this would hopefully provide the context for folding of the polypeptide into a specific structure suitable for crystallization.

Overexpression for the purpose of purification and biochemical analysis of a Rev1 fragment was also attempted as part of this study, but expression levels were low and the majority of the protein expressed was in an insoluble form. Clearly, the Rev1 fragment selected is unsuitable, and a new one will need to be selected or designed. A fragment encoding the C-terminal 238 amino acids, in addition to Rev1-CT150, was demonstrably able to interact with the Rad5 truncations in the Y2H assay, and could be a suitable alternative. However, examination of the sequence of the C-terminus of Rev1 utilizing BLAST indicates that sequence conservation in the region is greatest between residues 741 and 985 (the C-terminal 245 amino acids). A construct designed around this region of sequence conservation is again more likely to allow proper folding of a distinct structure appropriate for crystallization and structural studies.

## 4.4 Sequence Analysis of the Rev1 Interacting Domain of Rad5

An alternative approach to determine the key residues in Rad5 for the protein-protein interaction with Rev1 is to look at an alignment of Rad5 with homologous sequences. A BLAST search of the *S. cerevisiae* Rad5 sequence reveals that the N-terminus of the protein is poorly conserved particularly compared to its well conserved SWI/SNF2 ATPase and RING finger domains. However, the results of this study provide a framework to examine the region between residues 21-30 more closely for conservation of specific residues. Since the N-terminus of Rad5 is not widely conserved, comparison to homologues from relatively closely related organisms such as other fungi may provide a better context. The *Saccharomyces* genome database (http://www.yeastgenome.org/) has a fungal sequence alignment tool, and a section of the alignment of the amino acid sequence of Rad5 that this tool produces is shown in Figure 4.1. Based on these results, and a cursory examination of the BLAST results for Rad5, we predict that residues 24-27 (LNFK) may be the key residues for the interaction with Rev1. Mutations such as L24A or F26A would be suitable targets for abolishing the interaction of Rad5 with Rev1 without disrupting any other functions of Rad5. Future functional studies will be required to verify this hypothesis.

## 4.5 Analysis of a Potential TLS Deficient *rad5* Mutation

In order to assess the functional effects of any point mutations in Rad5 on the interaction between Rad5 and Rev1 it is important to first verify whether these mutations affect any other function of Rad5. Rad5 physically interacts with PCNA, Rad18 and Ubc13 (Carlile et al., 2009; Ulrich and Jentsch, 2000). Assessment of the effect of the point mutations on these interactions should determine whether they solely disrupt binding to Rev1. Furthermore, the

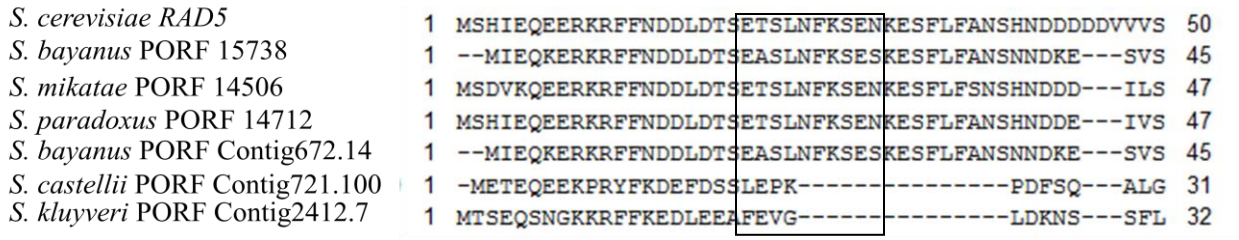


**Figure 4.1 – Rad5 N-terminus fungal sequence alignment.** The fungal sequence alignment was produced utilizing the tool on the *Saccharomyces* genome database (http://www.yeastgenome.org/cache/fungi/YLR032W.html) which uses the ClustalW alignment software. The box indicates the amino acids of interest located from position 21-30 that are suspected to contain the key residues for the interaction of Rad5 with Rev1. Amino acids 24-27 (LNFK) are suspected to serve as the key motif for Rev1 binding.

functional effects of the point mutations can be assessed by a complementation analysis in a *rad5Δ* strain of *S. cerevisiae* similar to the N-terminal deletion utilized in this study. The TLS activity of Rad5 is only important in TLS bypass of specific DNA lesions (Gangavarapu et al., 2006; Pages et al., 2008) and the sensitivity of TLS null mutants to DNA damaging agents is only slight compared to *rad5Δ* (Gangavarapu et al., 2006). Therefore, a TLS deficient *rad5* mutant should complement a *rad5* null mutant to a high degree, rescuing the sensitivity to DNA damaging agents to nearly wild-type levels. Since the region of Rad5 identified to interact with Rev1 here has not been associated with any other activities of the multifunctional Rad5 protein, it supports the possibility of the creation of a point mutation disrupting only the interaction with Rev1 and by extension the function Rad5 mediates in TLS.

Further analysis can be carried out on a putatively TLS deficient *rad5* mutant based on the synergistic and epistatic relationships that exist between the genes involved in DDT. Mutations disrupting the error-free branch of DDT, such as *mms2Δ* or *ubc13Δ*, result in a significantly higher sensitivity to DNA damaging agents than mutations in the TLS pathway, such as *rev3Δ* or *rev7Δ*. Combination of a mutation abolishing error-free DDT and one disabling TLS in the same strain results in a synergistic effect where the double mutant is significantly more sensitive to DNA damage than either single mutant (Broomfield et al., 1998; Brusky et al., 2000; Cejka et al., 2001; Xiao et al., 2000). Should a point mutation within *RAD5* disrupting the interaction with Rev1 also abolish its TLS activity as we expect, the point mutation would result in little sensitivity to DNA damaging agents unless combined with a mutation in the error-free branch of DDT, in which case a synergistic relationship would be revealed.

The TLS genes were identified primarily as *REV* genes, indicating their requirement for UV induced mutagenesis, and loss of a TLS gene results in loss of induced mutagenesis in

general (Lemontt, 1971). In contrast, mutations preventing the error-free mechanism of DDT result in elevated rates of mutagenesis, as it forces lesion bypass through the TLS route (Broomfield et al., 1998; Broomfield et al., 2001; Brusky et al., 2000; Xiao et al., 2000). Initial identification of the *REV* genes also identified *RAD5* as *REV2* based on its requirement for UV induced reversion of the *arg4-17* allele, specifically, and the gene is also required for TLS bypass of abasic sites and bulky adducts (Gangavarapu et al., 2006; Lemontt, 1971; Pages et al., 2008). However, it is not required for TLS bypass of other types of DNA damage during replication. Analysis of the UV induced reversion of the *arg4-17* allele in the putative TLS deficient *rad5* mutant compared to another TLS mutant will confirm whether the mutation abolishes the TLS role of Rad5 along with the interaction with Rev1.

Once a TLS *rad5* mutant is verified, it can be utilized to determine whether the TLS role of the protein accounts for the unknown function(s) in DDT. The multiple point mutations disrupting the ATPase activity, RING finger E3 activity and TLS activity can be combined and compared to a *rad5* null mutant. Provided these point mutations abolish all of Rad5's roles combined they will result in a similar sensitivity to DNA damaging agents as the null mutant. If Rad5 possesses yet more unidentified functions, the combined point mutations should be less sensitive to DNA damage, and more work will be required to uncover what these functions may be.

### 4.6 Genetic Placement of *RAD5* in DDT

While it is clear that the role of Rad5 in DDT has not been completely defined, it is still possible that it also functions in a cellular process outside of DDT. In order to define whether Rad5 acts solely within DDT its genetic relationships with components involved in the initial

activation of DDT were determined. Specifically, activation of DDT requires ubiquitination and sumoylation of the PCNA homotrimer, encoded by *POL30*, at K164 (Hoege et al., 2002). A K164R point mutation prevents these covalent modifications of PCNA, and activation of DDT, and as such this point mutation is epistatic to all other DDT mutants. Sumoylation of PCNA is required to recruit Srs2 which prevents inappropriate activation of HR that would otherwise interfere with DDT (Pfander et al., 2005). An *srs2* null mutation thus overcomes the sensitivity of DDT mutations by allowing repair attempts to be routed through HR and preventing initiation of DDT by the cell (Schiestl et al., 1990). Within DDT, Rad6 and Rad18 function as an E2-E3 complex for initial mono-ubiquitination of PCNA-K164 at sites of replication blocking DNA damage (Bailly et al., 1994; Ulrich and Jentsch, 2000). Loss of either therefore prevents activation of DDT and so both should be epistatic to all other genes downstream (Prakash et al., 1993). With these relationships in mind, the *rad5* null mutation was combined with *rad18Δ*, *srs2Δ* and *pol30-K164R* and assessed for sensitivity to killing by DNA damaging agents utilizing both qualitative and quantitative assays. A *rad6* mutation was not included in the experiments since *RAD6* is required for several important cellular processes, including N-end rule protein degradation and sporulation (Andersen et al., 2008; Prakash, 1994). If Rad5 acts solely within DDT, the double mutants would be expected to exhibit the same sensitivity to DNA damaging agents as the respective *rad18Δ*, *srs2Δ* or *pol30-K164R* single mutants.

Initial screening for DNA damage sensitivity was carried out in both the HK578 and DBY747 yeast strain backgrounds utilizing the serial dilution assay with MMS and UV as DNA damaging agents. Unexpectedly, the *rad5Δ rad18Δ* double mutant exhibited an additive phenotype when compared to the sensitivity of either single mutant, a phenotype which could indicate that *RAD5* may be involved in a cellular process other than DDT. However, both the

*rad5Δ srs2Δ* and *pol30-K164R rad5Δ* double mutants demonstrated an epistatic relationship compared to the respective single mutants. The results were consistent between yeast strain backgrounds and between the two different DNA damaging agents. The epistasis analysis was repeated utilizing gradient plate analysis, an alternative qualitative assay, in the HK578 strain background with MMS as the damaging agent, and the results were consistent with the serial dilution assays.

Both qualitative assays involve treatment with a relatively low dose of the DNA damaging agent over an extended period of time, while the quantitative liquid killing technique utilizes an acute dose over a short period of time. This assay was also utilized to examine the genetic placement of *RAD5* in DDT. In the HK578 background with MMS treatment, the liquid killing assay confirmed the results of the qualitative assessments. Interestingly, the additive relationship between *rad5Δ* and *rad18Δ* has been observed once previously with γ-radiation (Moertl et al., 2008). However, no research has been released to follow up on this phenotype which is not explained by the current model of DDT. The genetic relationships exhibited here indicate that *RAD5* and *RAD18* have functions independent of each other. However, *RAD5* functions in a manner dependent on PCNA modification, which implies a function solely within DDT. It is possible that *RAD18* may function outside of DDT, explaining its genetic relationship with *RAD5*, however, *RAD18* has a clear epistatic relationship with other genes involved in DDT (Broomfield et al., 1998). It is clear from these results, and the mounting evidence for Rad5 activities outside of the error-free branch of DDT, that our current model of DDT is incomplete, and further study is required to determine the exact relationships between the two branches and the mechanisms involved in DDT.

### 4.7 Implications of the Genetic Data

Two different approaches were utilized in this study to begin to determine the uncharacterized functions of the *S. cerevisiae* Rad5 protein. The first approach followed up on evidence for a role in the TLS branch of DDT, specifically aimed at understanding the physical interaction between Rad5 and Rev1, a TLS protein, and how it pertains to the TLS function of Rad5. The other approach was a more general examination of the genetic relationships between *RAD5* and genes involved in activation of DDT to rule out whether Rad5 may play a role in any other cellular processes. Interestingly, the genetic results were mixed, indicating the possibility of an activity of Rad5 perhaps outside of process of DDT itself, but dependent on PCNA modification, which is required for initiation of DDT (Hoege et al., 2002). This may indicate multiple uncharacterized functions for Rad5, one involved in mediating TLS, and another which is independent of *RAD18*.

It is possible, however, that the phenotype uncovered in the epistasis analysis of *rad5Δ* can be explained by the role of Rad5 in TLS. Rad5 physically interacts with PCNA, both in the absence and presence of mono-ubiquitinated PCNA, along with Rad18, Ubc13 and Rev1 (Carlile et al., 2009; Pages et al., 2008; Ulrich and Jentsch, 2000). While there is evidence for the involvement of Rad5 in TLS, it appears to be a partial activity, involved in mediating TLS bypass of specific types of damage (Pages et al., 2008). Additionally, there has been evidence that Rad5 has a ssDNA binding activity, associated with the ATPase domain (Johnson et al., 1994). Based on this information it is conceivable that in the absence of Rad18 and the initial ubiquitination of PCNA activating DDT, Rad5 is still capable of binding both PCNA and Rev1 and activating a limited level of TLS. Rev1 serves an important role not just as a deoxycytidilyl transferase, but also as a scaffolding protein for assembly of the other TLS polymerases (Prakash et al., 2005). Also, while Rev1 possesses a ubiquitin-binding motif, it has been proposed that

mono-ubiquitination of PCNA is not necessarily required for the recruitment of TLS proteins, but is instead more important for disrupting the association of potentially interfering proteins such as the replication machinery (Andersen et al., 2008; Sale et al., 2012). It is possible that Rad5 may be capable of partially activating the TLS pathway of DDT in a *rad18* null mutant through the recruitment of Rev1 to stalled replication forks. This could explain why the *rad5Δ rad18Δ* double mutant is more sensitive to killing by DNA damaging agents than the *rad18Δ* single mutant.

A simple method to determine whether Rad5 can partially activate TLS in *rad18Δ* background would be to directly compare the sensitivity of a *rev1Δ rad18Δ* double mutant to the *rad5Δ rad18Δ* double mutant and *rad18Δ* single mutant. If Rad5 is activating TLS through the recruitment of Rev1 to a stalled replication fork in the absence of mono-ubiquitinated PCNA, the proposed double mutants should exhibit identical sensitivities to DNA damaging agents, which are slightly higher than the sensitivity of a *rad18* null mutant. If this hypothesis is incorrect, the *rev1Δ rad18Δ* double mutant should more closely resemble the *rad18Δ* single mutant than *rad5Δ rad18Δ*.

An alternative explanation for the phenotypes observed in the epistasis analysis is that Rad5 may be involved in sumoylation of PCNA or the downstream process dependent on sumoylation. Relevantly, a screen for protein interactions between yeast Srs2 and other yeast proteins indicates a potential interaction between Rad5 and Srs2 (Marini and Krejci, 2010). The interaction has not been confirmed, but it indicates a potential involvement for Rad5 in a process involving Srs2, perhaps related to the regulation of HR in the cell. One study of Rad5 suggested its involvement in double strand break repair in *S. cerevisiae*, a process typically attributed to HR repair (Ahne et al., 1997), which could be related to a role of Rad5 downstream of PCNA

sumoylation. Regardless, the current model of DDT and our understanding of its components are clearly incomplete.

### 4.8 Significance of These Research Findings

The identification of a small putative Rev1 binding domain within Rad5 provides a framework to further the understanding of the role of the physical interaction between Rad5 and Rev1 in the context of DDT and its different mechanisms. The identified region provides a target sequence for analysis of conservation and identification of key residues in a region of the protein that is not well conserved overall. Additionally, it provides a target region of the protein small enough to be considered for structural studies utilizing X-ray crystallography unlike the full length protein. Once the likely key residues are identified for the physical interaction, they can be specifically targeted for point mutations and functional analysis. This study also approached the problem of identifying the uncharacterized roles of the *S. cerevisiae* protein from a more general genetic approach. The genetic relationships between *rad5Δ* and several genes required for the activation of DDT in the cell were analyzed, and a unique relationship was discovered between *RAD5* and *RAD18*. However, the rest of the results indicate that the functions of Rad5 depend on the covalent modification of PCNA required for activation of DDT. This data indicates that the current model of DDT is not entirely complete, and further study is required to tease out the exact processes involved in this important DNA damage bypass mechanism and their impact on the field of cancer research.

# REFERENCES


Ahne, F., Jha, B., and Eckardt-Schupp, F. (1997). The RAD5 gene product is involved in the avoidance of non-homologous end-joining of DNA double strand breaks in the yeast Saccharomyces cerevisiae. Nucleic Acids Res *25*, 743-749.

Andersen, P.L., Xu, F., and Xiao, W. (2008). Eukaryotic DNA damage tolerance and translesion synthesis through covalent modifications of PCNA. Cell Res *18*, 162-173.

Bailly, V., Lamb, J., Sung, P., Prakash, S., and Prakash, L. (1994). Specific complex formation between yeast RAD6 and RAD18 proteins: a potential mechanism for targeting RAD6 ubiquitin-conjugating activity to DNA damage sites. Genes Dev *8*, 811-820.

Bailly, V., Lauder, S., Prakash, S., and Prakash, L. (1997). Yeast DNA repair proteins Rad6 and Rad18 form a heterodimer that has ubiquitin conjugating, DNA binding, and ATP hydrolytic activities. J Biol Chem *272*, 23360-23365.

Ball, L.G. (2011). A large scale genomic screen reveals mechanisms of yeast postreplication repair in Saccharomyces cerevisiae. In Microbiology and Immunology (Saskatoon, University of Saskatchewan).

Ball, L.G., Zhang, K., Cobb, J.A., Boone, C., and Xiao, W. (2009). The yeast Shu complex couples error-free post-replication repair to homologous recombination. Mol Microbiol *73*, 89-102.

Barbour, L., and Xiao, W. (2006). Mating type regulation of cellular tolerance to DNA damage is specific to the DNA post-replication repair and mutagenesis pathway. Mol Microbiol *59*, 637-650.

Bernstein, K.A., Reid, R.J., Sunjevaric, I., Demuth, K., Burgess, R.C., and Rothstein, R. (2011). The Shu complex, which contains Rad51 paralogues, promotes DNA repair through inhibition of the Srs2 anti-recombinase. Mol Biol Cell *22*, 1599-1607.

Blastyak, A., Pinter, L., Unk, I., Prakash, L., Prakash, S., and Haracska, L. (2007). Yeast Rad5 protein required for postreplication repair has a DNA helicase activity specific for replication fork regression. Mol Cell *28*, 167-175.

Branzei, D., Vanoli, F., and Foiani, M. (2008). SUMOylation regulates Rad18-mediated template switch. Nature *456*, 915-920.

Bridges, B.A., and Munson, R.J. (1968). Mutagenesis in Escherichia coli: evidence for the mechanism of base change mutation by ultraviolet radiation in a strain deficient in excision-repair. Proc R Soc Lond B Biol Sci *171*, 213-226.

Broomfield, S., Chow, B.L., and Xiao, W. (1998). MMS2, encoding a ubiquitin-conjugating-enzyme-like protein, is a member of the yeast error-free postreplication repair pathway. Proc Natl Acad Sci U S A *95*, 5678-5683.

Broomfield, S., Hryciw, T., and Xiao, W. (2001). DNA postreplication repair and mutagenesis in Saccharomyces cerevisiae. Mutat Res *486*, 167-184.

Brusky, J., Zhu, Y., and Xiao, W. (2000). UBC13, a DNA-damage-inducible gene, is a member of the error-free postreplication repair pathway in Saccharomyces cerevisiae. Curr Genet *37*, 168-174.

Carlile, C.M., Pickart, C.M., Matunis, M.J., and Cohen, R.E. (2009). Synthesis of free and proliferating cell nuclear antigen-bound polyubiquitin chains by the RING E3 ubiquitin ligase Rad5. J Biol Chem *284*, 29326-29334.

Ceballos, S.J., and Heyer, W.D. (2011). Functions of the Snf2/Swi2 family Rad54 motor protein in homologous recombination. Biochim Biophys Acta *1809*, 509-523.

Cejka, P., Vondrejs, V., and Storchova, Z. (2001). Dissection of the functions of the Saccharomyces cerevisiae RAD6 postreplicative repair group in mutagenesis and UV sensitivity. Genetics *159*, 953-963.
Deshaies, R.J., and Joazeiro, C.A. (2009). RING domain E3 ubiquitin ligases. Annu Rev Biochem *78*, 399-434.
Eisen, J.A., Sweder, K.S., and Hanawalt, P.C. (1995). Evolution of the SNF2 family of proteins: subfamilies with distinct sequences and functions. Nucleic Acids Res *23*, 2715-2723.
Fields, S., and Song, O. (1989). A novel genetic system to detect protein-protein interactions. Nature *340*, 245-246.
Friedberg, E.C. (1988). Deoxyribonucleic acid repair in the yeast Saccharomyces cerevisiae. Microbiol Rev *52*, 70-102.
Friedberg, E.C., Walker, G.C., Siede, W., and Schultz, R.A. (2006). DNA repair and mutagenesis, 2nd edn (Washington, ASM Press).
Ganesan, A.K. (1974). Persistence of pyrimidine dimers during post-replication repair in ultraviolet light-irradiated Escherichia coli K12. J Mol Biol *87*, 103-119.
Gangavarapu, V., Haracska, L., Unk, I., Johnson, R.E., Prakash, S., and Prakash, L. (2006). Mms2-Ubc13-dependent and -independent roles of Rad5 ubiquitin ligase in postreplication repair and translesion DNA synthesis in Saccharomyces cerevisiae. Mol Cell Biol *26*, 7783-7790.
Gareau, J.R., and Lima, C.D. (2010). The SUMO pathway: emerging mechanisms that shape specificity, conjugation and recognition. Nat Rev Mol Cell Biol *11*, 861-871.
Hochstrasser, M. (1996). Ubiquitin-dependent protein degradation. Annu Rev Genet *30*, 405-439.
Hoege, C., Pfander, B., Moldovan, G.L., Pyrowolakis, G., and Jentsch, S. (2002). RAD6-dependent DNA repair is linked to modification of PCNA by ubiquitin and SUMO. Nature *419*, 135-141.
Hoffman, C.S., and Winston, F. (1987). A ten-minute DNA preparation from yeast efficiently releases autonomous plasmids for transformation of Escherichia coli. Gene *57*, 267-272.
Hofmann, R.M., and Pickart, C.M. (1999). Noncanonical MMS2-encoded ubiquitin-conjugating enzyme functions in assembly of novel polyubiquitin chains for DNA repair. Cell *96*, 645-653.
Ito, H., Fukuda, Y., Murata, K., and Kimura, A. (1983). Transformation of intact yeast cells treated with alkali cations. J Bacteriol *153*, 163-168.
Iyer, L.M., Babu, M.M., and Aravind, L. (2006). The HIRAN domain and recruitment of chromatin remodeling and repair activities to damaged DNA. Cell Cycle *5*, 775-782.
James, P., Halladay, J., and Craig, E.A. (1996). Genomic libraries and a host strain designed for highly efficient two-hybrid selection in yeast. Genetics *144*, 1425-1436.
Jentsch, S., McGrath, J.P., and Varshavsky, A. (1987). The yeast DNA repair gene RAD6 encodes a ubiquitin-conjugating enzyme. Nature *329*, 131-134.
Johnson, E.S., and Blobel, G. (1997). Ubc9p is the conjugating enzyme for the ubiquitin-like protein Smt3p. J Biol Chem *272*, 26799-26802.
Johnson, R.E., Henderson, S.T., Petes, T.D., Prakash, S., Bankmann, M., and Prakash, L. (1992). Saccharomyces cerevisiae RAD5-encoded DNA repair protein contains DNA helicase and zinc-binding sequence motifs and affects the stability of simple repetitive sequences in the genome. Mol Cell Biol *12*, 3807-3818.

Johnson, R.E., Kondratick, C.M., Prakash, S., and Prakash, L. (1999). hRAD30 mutations in the variant form of xeroderma pigmentosum. Science *285*, 263-265.
Johnson, R.E., Prakash, S., and Prakash, L. (1994). Yeast DNA repair protein RAD5 that promotes instability of simple repetitive sequences is a DNA-dependent ATPase. J Biol Chem *269*, 28259-28262.
Johnson, R.E., Washington, M.T., Haracska, L., Prakash, S., and Prakash, L. (2000). Eukaryotic polymerases iota and zeta act sequentially to bypass DNA lesions. Nature *406*, 1015-1019.
Koken, M.H., Reynolds, P., Jaspers-Dekker, I., Prakash, L., Prakash, S., Bootsma, D., and Hoeijmakers, J.H. (1991). Structural and functional conservation of two human homologs of the yeast DNA repair gene RAD6. Proc Natl Acad Sci U S A *88*, 8865-8869.
Krejci, L., Van Komen, S., Li, Y., Villemain, J., Reddy, M.S., Klein, H., Ellenberger, T., and Sung, P. (2003). DNA helicase Srs2 disrupts the Rad51 presynaptic filament. Nature *423*, 305-309.
Kuang, L., Kou, H., Xie, Z., Zhou, Y., Feng, X., Wang, L., and Wang, Z. (2013). A non-catalytic function of Rev1 in translesion DNA synthesis and mutagenesis is mediated by its stable interaction with Rad5. DNA Repair (Amst) *12*, 27-37.
Laterjet, R., and Ephrussi, B. (1949). Courbes de survie de levures haloides et diploides soumises aux rayon X. C R Acad Sci *229*, 306-308.
Lawrence, C.W., Das, G., and Christensen, R.B. (1985). REV7, a new gene concerned with UV mutagenesis in yeast. Mol Gen Genet *200*, 80-85.
Lemontt, J.F. (1971). Mutants of yeast defective in mutation induced by ultraviolet light. Genetics *68*, 21-33.
Lorick, K.L., Jensen, J.P., Fang, S., Ong, A.M., Hatakeyama, S., and Weissman, A.M. (1999). RING fingers mediate ubiquitin-conjugating enzyme (E2)-dependent ubiquitination. Proc Natl Acad Sci U S A *96*, 11364-11369.
Maniatas, T., Fritsch, E.F., and Sambrook, J. (1989). Molecular cloning: a laboratory manual (Cold Spring Harbor, New York, Cold Spring Harbor Laboratory).
Mankouri, H.W., Ngo, H.P., and Hickson, I.D. (2007). Shu proteins promote the formation of homologous recombination intermediates that are processed by Sgs1-Rmi1-Top3. Mol Biol Cell *18*, 4062-4073.
Marini, V., and Krejci, L. (2010). Srs2: the "Odd-Job Man" in DNA repair. DNA Repair (Amst) *9*, 268-275.
Masutani, C., Kusumoto, R., Yamada, A., Dohmae, N., Yokoi, M., Yuasa, M., Araki, M., Iwai, S., Takio, K., and Hanaoka, F. (1999). The XPV (xeroderma pigmentosum variant) gene encodes human DNA polymerase eta. Nature *399*, 700-704.
McDonald, J.P., Levine, A.S., and Woodgate, R. (1997). The Saccharomyces cerevisiae RAD30 gene, a homologue of Escherichia coli dinB and umuC, is DNA damage inducible and functions in a novel error-free postreplication repair mechanism. Genetics *147*, 1557-1568.
Minca, E.C., and Kowalski, D. (2010). Multiple Rad5 activities mediate sister chromatid recombination to bypass DNA damage at stalled replication forks. Mol Cell *38*, 649-661.
Moertl, S., Karras, G.I., Wismuller, T., Ahne, F., and Eckardt-Schupp, F. (2008). Regulation of double-stranded DNA gap repair by the RAD6 pathway. DNA Repair (Amst) *7*, 1893-1906.
Nakai, S., and Matsumoto, S. (1967). Two types of radiation-sensitive mutant in yeast. Mutat Res *4*, 129-136.
Nelson, J.R., Lawrence, C.W., and Hinkle, D.C. (1996). Deoxycytidyl transferase activity of yeast REV1 protein. Nature *382*, 729-731.

Pages, V., Bresson, A., Acharya, N., Prakash, S., Fuchs, R.P., and Prakash, L. (2008). Requirement of Rad5 for DNA polymerase zeta-dependent translesion synthesis in Saccharomyces cerevisiae. Genetics *180*, 73-82.
Parker, J.L., and Ulrich, H.D. (2009). Mechanistic analysis of PCNA poly-ubiquitylation by the ubiquitin protein ligases Rad18 and Rad5. Embo J *28*, 3657-3666.
Pfander, B., Moldovan, G.L., Sacher, M., Hoege, C., and Jentsch, S. (2005). SUMO-modified PCNA recruits Srs2 to prevent recombination during S phase. Nature *436*, 428-433.
Pickart, C.M. (1997). Targeting of substrates to the 26S proteasome. Faseb J *11*, 1055-1066.
Pickart, C.M. (2000). Ubiquitin in chains. Trends Biochem Sci *25*, 544-548.
Prakash, L. (1981). Characterization of postreplication repair in Saccharomyces cerevisiae and effects of rad6, rad18, rev3 and rad52 mutations. Mol Gen Genet *184*, 471-478.
Prakash, L. (1994). The RAD6 gene and protein of Saccharomyces cerevisiae. Ann N Y Acad Sci *726*, 267-273.
Prakash, L., and Prakash, S. (1977). Isolation and characterization of MMS-sensitive mutants of Saccharomyces cerevisiae. Genetics *86*, 33-55.
Prakash, S., Johnson, R.E., and Prakash, L. (2005). Eukaryotic translesion synthesis DNA polymerases: specificity of structure and function. Annu Rev Biochem *74*, 317-353.
Prakash, S., and Prakash, L. (2002). Translesion DNA synthesis in eukaryotes: a one- or two-polymerase affair. Genes Dev *16*, 1872-1883.
Prakash, S., Sung, P., and Prakash, L. (1993). DNA repair genes and proteins of Saccharomyces cerevisiae. Annu Rev Genet *27*, 33-70.
Sale, J.E., Lehmann, A.R., and Woodgate, R. (2012). Y-family DNA polymerases and their role in tolerance of cellular DNA damage. Nat Rev Mol Cell Biol *13*, 141-152.
Saurin, A.J., Borden, K.L., Boddy, M.N., and Freemont, P.S. (1996). Does this have a familiar RING? Trends Biochem Sci *21*, 208-214.
Serebriiskii, I.G., Milech, N., and Golemis, E. A. (2000). A bacterial/yeast merged two-hybrid system: protocol for bacterial screening. Methods Mol Biol *408*, 291-315.
Schiestl, R.H., Prakash, S., and Prakash, L. (1990). The SRS2 suppressor of rad6 mutations of Saccharomyces cerevisiae acts by channeling DNA lesions into the RAD52 DNA repair pathway. Genetics *124*, 817-831.
Schwartz, D.C., and Hochstrasser, M. (2003). A superfamily of protein tags: ubiquitin, SUMO and related modifiers. Trends Biochem Sci *28*, 321-328.
Spence, J., Sadis, S., Haas, A.L., and Finley, D. (1995). A ubiquitin mutant with specific defects in DNA repair and multiubiquitination. Mol Cell Biol *15*, 1265-1273.
Stelter, P., and Ulrich, H.D. (2003). Control of spontaneous and damage-induced mutagenesis by SUMO and ubiquitin conjugation. Nature *425*, 188-191.
Tang, L., Nogales, E., and Ciferri, C. (2010). Structure and function of SWI/SNF chromatin remodeling complexes and mechanistic implications for transcription. Prog Biophys Mol Biol *102*, 122-128.
Torres-Ramos, C.A., Yoder, B.L., Burgers, P.M., Prakash, S., and Prakash, L. (1996). Requirement of proliferating cell nuclear antigen in RAD6-dependent postreplicational DNA repair. Proc Natl Acad Sci U S A *93*, 9676-9681.
Ulrich, H.D. (2003). Protein-protein interactions within an E2-RING finger complex. Implications for ubiquitin-dependent DNA damage repair. J Biol Chem *278*, 7051-7058.
Ulrich, H.D. (2011). Timing and spacing of ubiquitin-dependent DNA damage bypass. FEBS Lett *585*, 2861-2867.

Ulrich, H.D., and Jentsch, S. (2000). Two RING finger proteins mediate cooperation between ubiquitin-conjugating enzymes in DNA repair. Embo J *19*, 3388-3397.
Unk, I., Hajdu, I., Blastyak, A., and Haracska, L. (2010). Role of yeast Rad5 and its human orthologs, HLTF and SHPRH in DNA damage tolerance. DNA Repair (Amst) *9*, 257-267.
Unk, I., Hajdu, I., Fatyol, K., Hurwitz, J., Yoon, J.H., Prakash, L., Prakash, S., and Haracska, L. (2008). Human HLTF functions as a ubiquitin ligase for proliferating cell nuclear antigen polyubiquitination. Proc Natl Acad Sci U S A *105*, 3768-3773.
Unk, I., Hajdu, I., Fatyol, K., Szakal, B., Blastyak, A., Bermudez, V., Hurwitz, J., Prakash, L., Prakash, S., and Haracska, L. (2006). Human SHPRH is a ubiquitin ligase for Mms2-Ubc13-dependent polyubiquitylation of proliferating cell nuclear antigen. Proc Natl Acad Sci U S A *103*, 18107-18112.
VanDemark, A.P., Hofmann, R.M., Tsui, C., Pickart, C.M., and Wolberger, C. (2001). Molecular insights into polyubiquitin chain assembly: crystal structure of the Mms2/Ubc13 heterodimer. Cell *105*, 711-720.
Veaute, X., Jeusset, J., Soustelle, C., Kowalczykowski, S.C., Le Cam, E., and Fabre, F. (2003). The Srs2 helicase prevents recombination by disrupting Rad51 nucleoprotein filaments. Nature *423*, 309-312.
Welchman, R.L., Gordon, C., and Mayer, R.J. (2005). Ubiquitin and ubiquitin-like proteins as multifunctional signals. Nat Rev Mol Cell Biol *6*, 599-609.
Xiao, W., Chow, B.L., Broomfield, S., and Hanna, M. (2000). The Saccharomyces cerevisiae RAD6 group is composed of an error-prone and two error-free postreplication repair pathways. Genetics *155*, 1633-1641.
Xiao, W., Chow, B.L., Fontanie, T., Ma, L., Bacchetti, S., Hryciw, T., and Broomfield, S. (1999). Genetic interactions between error-prone and error-free postreplication repair pathways in Saccharomyces cerevisiae. Mutat Res *435*, 1-11.
Yu, S., Teng, Y., Waters, R., and Reed, S.H. (2011). How chromatin is remodelled during DNA repair of UV-induced DNA damage in Saccharomyces cerevisiae. PLoS Genet *7*, e1002124.
Zhang, H., and Lawrence, C.W. (2005). The error-free component of the RAD6/RAD18 DNA damage tolerance pathway of budding yeast employs sister-strand recombination. Proc Natl Acad Sci U S A *102*, 15954-15959.
Zhang, H., and Siede, W. (2002). UV-induced T-->C transition at a TT photoproduct site is dependent on Saccharomyces cerevisiae polymerase eta in vivo. Nucleic Acids Res *30*, 1262-1267.
Zhang, W., Qin, Z., Zhang, X., and Xiao, W. (2011). Roles of sequential ubiquitination of PCNA in DNA-damage tolerance. FEBS Lett *585*, 2786-2794.